# Uplift Capacity of Battered Piles in Sand

Alfred Afram

A Thesis

in

The Department

of

Civil Engineering

Presented in Partial Fulfillment of the Requirements
for the Degree of Master of Engineering at
Concordia University
Montréal, Québec, Canada

November 1984

# ABSTRACT

## Uplift Capacity of Battered Piles in Sand

Alfred Afram

Foundations subjected to moment and uplift loads such as transmission towers and offshore structures are usually supported on a system of vertical and battered piles.

The present experimental investigation is to study the effect of pile size and pile inclination on the ultimate uplift capacity of a single battered pile in sand.

The results of model tests on 1½ and 3 inches piles are analyzed and design theory and charts are developed. For vertical piles, the experimental results have showed good agreement with Meyerhof's theory while for battered piles a new theory was developed.

## ACKNOWLEDGEMENT

The author wishes to express his sincere appreciation to Dr. A.M. Hanna, under whose supervision, guidance and fruitful suggestions this work was carried out.

Credit is also due to Mr. T.Q. Nguyen for his design of the experimental set-up and his continuous support and cooperation; Mr. R. Lombardo for his technical assistance and helpful ideas; and to Mrs. Paulette Vigneault for her judicious typing of the entire manuscript.

The author is grateful to the National Science and Engineering Council of Canada for the financial assistance.

Last, but not least, the author wishes to dedicate this thesis to his wife, Rita, for her help, encouragement and understanding throughout the course of his work.

# TABLE OF CONTENTS

## LIST OF SYMBOLS

| | |
|---|---|
| $A'$ | Adjusted Area |
| $C_u$ | Coefficient of Uniformity |
| $D$ | Diameter of Pile |
| $D_{10}$ | Size such that 10% of particles are smaller |
| $D_{60}$ | Size such that 60% of particles are smaller |
| $e$ | Void Ratio |
| $e_{max}, e_{min}$ | Maximum and Minimum Void Ratio |
| $F$ | Friction force mobilized on curved failure surface |
| $F_s$ | Frictional Resistance |
| $G_s$ | Specific Gravity of Sand |
| $K$ | Coefficient of Earth Pressure |
| $K_o$ | Coefficient of Earth Pressure at Rest |
| $K_p, K_a$ | Passive and Active Coefficients of Earth Pressure |
| $K_u$ | Uplift Coefficient |
| $K_n$ | Lateral Pressure Constant |
| $L$ | Length of Pile |
| $N$ | Number of blows using Standard Penetration Test |
| NC | National Coarse |
| $P_u$ | Gross ultimate Uplift Capacity |
| $P_p$ | Total passive earth pressure inclined at average angle . |

| | |
|---|---|
| $P_o$ | Net Ultimate Uplift Capacity of Vertical Pile |
| P.R | Proving Ring |
| $P_\alpha$ | Net Ultimate Uplift Capacity of inclined pile |
| Q | Uplift capacity of Pile |
| q | Surcharge |
| R.D | Relative Density |
| $t_f$ | Unit Shearing Resistance |
| UNF | Uniform National Fine |
| $W_p$ | Weight of Pile |
| $W_c$ | Weight of Concrete Pile |
| W | Effective Weight of Shaft |
| Z | Depth of Center of Gravity of Embedded Pile |
| $\alpha$ | Angle of Inclination of Pile |
| $\alpha_1$ | Average Inclination of Force F with Vertical |
| $\gamma_w$ | Unit Weight of Water |
| $\gamma_d$ | Dry Unit Weight of Soil |
| $\gamma$ | Unit Weight of Soil |
| $\gamma'$ | Effective Unit Weight of Soil |
| $\sigma, \sigma_n$ | Normal Stress on Failure Surface |
| $\sigma_1, \sigma_3$ | Total Principal Stresses |
| $\mu$ | Coefficient of Friction |
| $\phi$ | Angle of Internal Friction |
| $\phi'$ | Effective Angle of Internal Friction |
| $\tau_{max}$ | Shear Stress |
| $\delta$ | Average angle of inclination for the Total passive earth pressure. |

## LIST OF FIGURES

# LIST OF TABLES

# CHAPTER I

## INTRODUCTION

In the design of structures subjected to overturning moments, it is necessary to evaluate the resistance of the foundations to uplifting loads. This is of particular importance in the design of transmission and radio towers and many off-shore structures (Fig. 1.1).

The resistance of soil to compression is reasonably well understood; however, the resistance to uplift is uncertain. Moreover, for piles of uniform diameter in sand there is little information available for evaluating the skin friction for upward loading and it is to some extent conflicting. Very little was reported in the literature about the ultimate uplift capacity of battered piles in sand under axial pull.

Thus large scale experimental tests on battered piles in uniform sand are planned to study the influence of pile size and pile inclination on the ultimate uplift capacity of vertical and inclined piles subjected to axial loads.

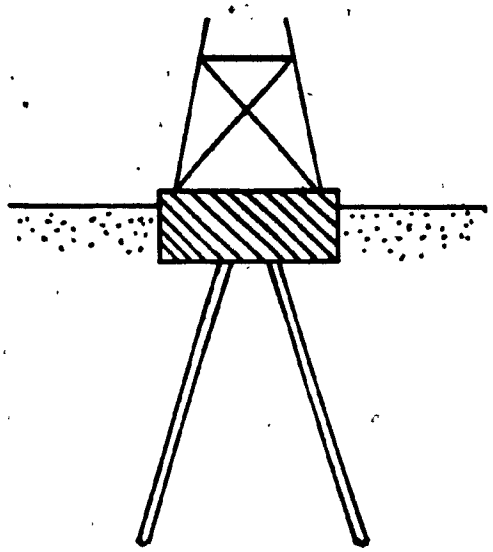

A TRANSMISSION TOWER FOUNDATION

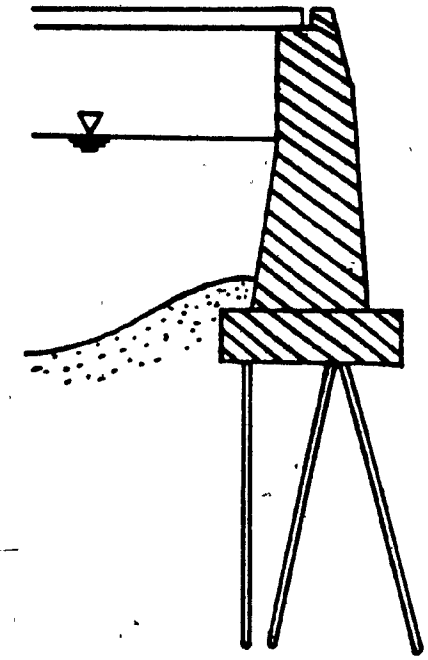

A BRIDGE ABUTMENT FOUNDATION

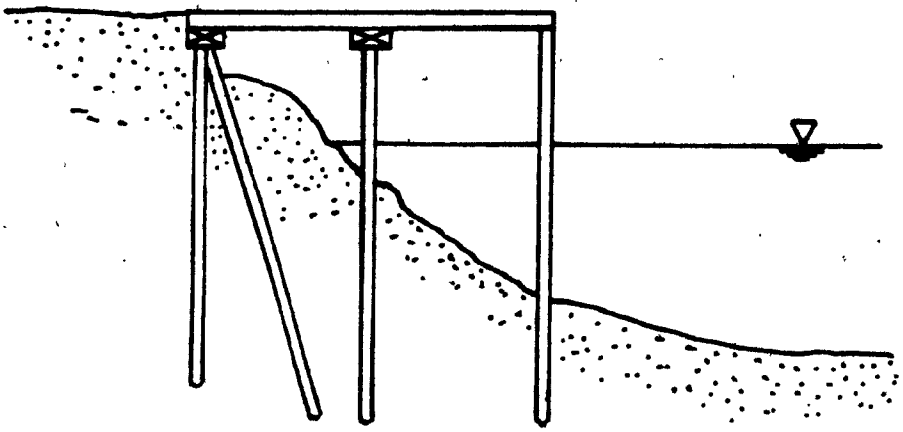

A FOUNDATION ON PILES FOR WHARFS.

FIGURE 1.1 - EXAMPLES OF THE USE OF BATTERED PILES SUBJECTED TO UPLIFT LOADS.

## SCOPE OF THE THESIS

After writing the introduction in Chapter I, the historical background on the subject will be discussed in chapter II. Laboratory set-up and properties of the materials used in this investigation are discussed in chapter III. The experimental results are tabulated and graphed in chapter IV. Chapter V will present the analysis of the present test results and any other available data. Finally, a conclusion and recommendations for future research on the subject will be given in chapter VI.

# CHAPTER II

## HISTORICAL BACKGROUND

Published large-scale field test results for the pull-out capacity of battered piles in uniform sand are relatively scarce. A limited amount of work is found in literature regarding the theoretical and experimental determinations of the uplift capacity of pile foundations in granular soils.

Ireland (10) as early as 1957 carried out many pulling large scale field tests on cast-in-place Raymond step-taper piles driven into fine sand. The field tests reported in his study indicate that the shearing resistance developed on a single pile in sand may approach that corresponding to a passive state of stress. The coefficient of earth pressure, K, in Ireland's equation is at least 1.75.

The equation is expressed as:

$$P_o = \pi DL\ (\gamma Z + q)\ K \tan\phi \qquad 2.1$$

in which Z is the depth of center of gravity of the embedded portion of pile i.e. $Z = L/2$. When the ground surface is not subjected to surcharge q, the equation is expressed as follows:

$$P_o = 1/2\ \pi D L^2 \gamma K \tan\phi \qquad 2.2$$

$\tan\phi$ represents the coefficient of friction in case of rough pile.

Vierendeel published a static formula for friction pile in dry sand that was identified by Jumikis (12). His equation is based on the Rankine's theory of earth pressure. The ultimate skin friction along the pile surface is determined by the following equation:

$$P_o = 1/2\ \pi D L^2\ \gamma \mu \tan^2 (45 + \phi/2) \qquad 2.3$$

in which $\mu$ is the coefficient of friction, it is equal to 0.33 for cast-in-place and concrete piles with rough surface and 0.25 for all other piles. But these static formulas are based on the assumption that the uplift resistance is equal to the resistance of friction between the cohesionless soil and the pile surface. Moreover this resistance of friction is approximately the same for both compression and tension piles.

If static-cone-penetration tests are used as a basis for estimating ultimate uplift skin resistance, Begemann (2) suggests that the maximum pulling force and the distribution of adhesion along the pile can be considerably affected by whether the load is applied continuously or with considerable fluctuations.

According to Begemann the calculated skin resistance should be adjusted by a reduction factor dependant on the soil and pile type (Fig. 2.1). However, these factors should be used with considerable caution as they are based on limited data.

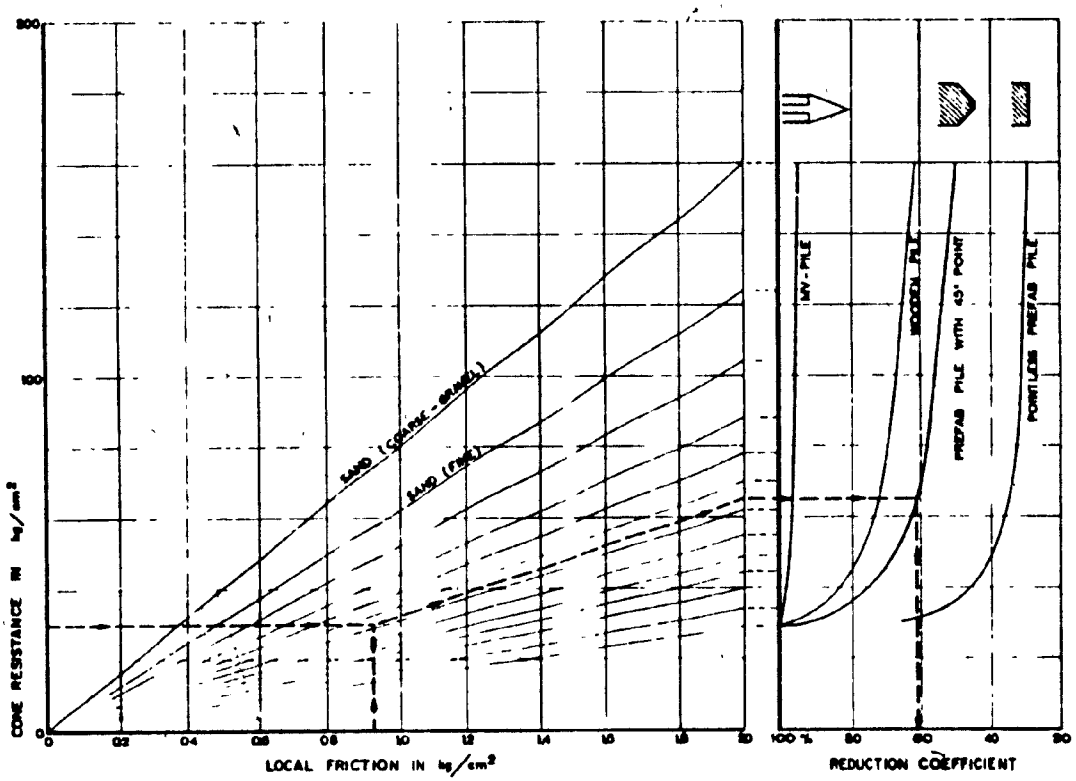


Fig. 2.1. Reduction curves for calculating friction along tension piles.

Downs and Chieurzzi (9) also tried to evaluate the uplift capacity of cased cylindrical piles where the frictional resistance depends on the lateral soil pressure acting normal to the pile (Fig. 2.2). Mathematical relationships are as follows:

$$Q = F_s + W_c \qquad 2.4$$

$$F_s = \frac{\pi DL}{2} \left(K_n \gamma_s L \tan\phi\right) \qquad 2.5$$

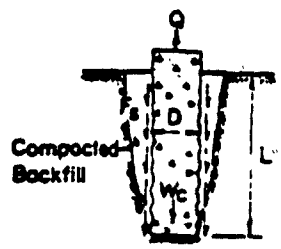


Fig. 2.2 Uplift Capacity of cased cylindrical piles

Where $F_s$ = Frictional Resistance

$\gamma_s$ = Unit weight of soil.

$\phi$ = Angle of Internal Friction

& $K_n$ = lateral pressure constant.

The results show that the uplift capacity varies with the degree of compaction and length of footing and that corrugated casing provides a greater resistance to uplift than does smooth casing. The values of the constant ($K_n$) are summarized in Table (2.1), and appear to reflect type of casing and method of backfill compaction; however, the correlations are not consistent. Further testing is necessary before reliable design criteria may be developed.

## SUMMARY OF Kn VALUES FOR CASED FOOTINGS

| Footing No. | Kn | Description |
|---|---|---|
| 1 | 0.82 | Corrugated Casing (10' long) Flooded Sand Backfill |
| 2 | 1.03 | Vibrated Sand Backfill of 1 |
| 3 | 1.45 | Drove Mandrels Around 2 and Tamped Sand Into Holes Left by Removal of Mandrels |
| 4 | 1.03 | Same as 1, Except 15' long |
| 5 | 0.91 | Same as 2, Except 15' long |
| 6 | 1.22 | Same as 3, Except 15' long |
| 7 | 0.44 | Corrugated Casing (10' long) Backfilled by Caving Native Wet Sand |
| 8 | 0.55 | Vibrated Sand Backfill of 7 |
| 9 | 1.69 | Drove Mandrels Around 8 |
| 10 | 0.38 | Same as 7, Except Smooth Casing |
| 11 | 0.28 | Same as 8, Except Smooth Casing |
| 12 | 0.75 | Same as 9, Except Smooth Casing |

TABLE 2.1

According to Sowa (22), the pulling capacity of vertical piles in sandy soil is very much dependent on the effective lateral pressure on the piles. The coefficient of lateral pressure, K, can vary over a wide range of values and is very sensitive to small values of cohesion. Based on the significant scatter of the K values, Sowa has indicated that it is difficult to select a suitable value of K, even for preliminary design purposes. Pile pulling tests are required therefore at the outset to establish the pulling capacity and skin friction of cast-in-situ piles in sandy soils.

Vesic (25) after comparing the ultimate load of the test pile in tension with the ultimate skin load of the same pile in compression, concluded that the ultimate skin loads in tension and compression are the same. But ultimate skin loads in laboratory tests of vertical piles (2" diam.) under axial pull load indicate a value as small as 30% of the ultimate skin loads in compression. Vesic attributed this apparent discrepancy to scale effects.

Meyerhof (15) was the first to attempt calculating the uplift capacity of inclined piles under axial pull. It was concluded that the uplift resistance can be expressed in terms of uplift coefficients (Fig. 2.3) which

have been evaluated by extending the previous theory for vertical uplift of foundations. Accordingly for piles under axial pull with a given depth of embedment and method of installation, the unit skin friction in uniform sand does not vary significantly for pile inclinations of less than 45°.

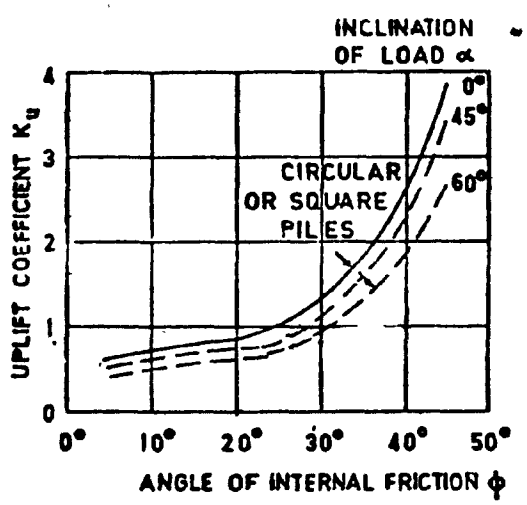


Fig. 23. Theoretical Uplift Coefficients for Bored Piles.

Laboratory model tests were conducted by Das and Seeley (8) to study the ultimate capacity of vertical piles under axial pull. Based on their results they concluded that the variation of unit uplift skin friction for piles is approximately linear with depth up to a critical embedment ratio beyond which it reaches a limiting value. While critical depth is established for compression,

it must be viewed with considerable caution in case of uplift resistance of piles because there is no experimental evidence to it.

For short rigid piles the uplift capacity can be calculated by using Meyerhof's uplift coefficients.

Ayoud and Awad (1) presented some model test results on the ultimate uplift capacity of vertical and inclined piles under axial pull. The results indicated that the ultimate uplift capacity of inclined piles decreases by increasing the angle of inclination as shown in Fig. (2.4). Moreover by applying Vierendeel's equation (2.3) a good agreement was obtained between the computed values and the experimental ones. If the pile is not too much inclined ($\alpha < 30^{o}$), it is suggested that the net ultimate uplift capacity of inclined piles can be computed by the empirical equation:

$$P_{\alpha} = P_{o} \frac{\cos \alpha}{\cos \alpha + \tan \alpha} \qquad 2.6$$

in which $P_o$ is the net ultimate capacity of vertical piles as computed by Ireland. By applying this equation, a good agreement was obtained as shown in Fig. (2.5)

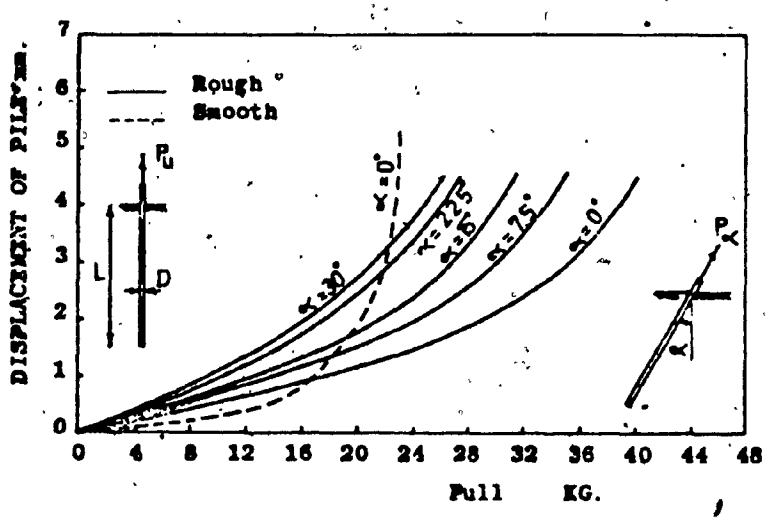


Fig.2.4. Pull load versus diplacement of pile

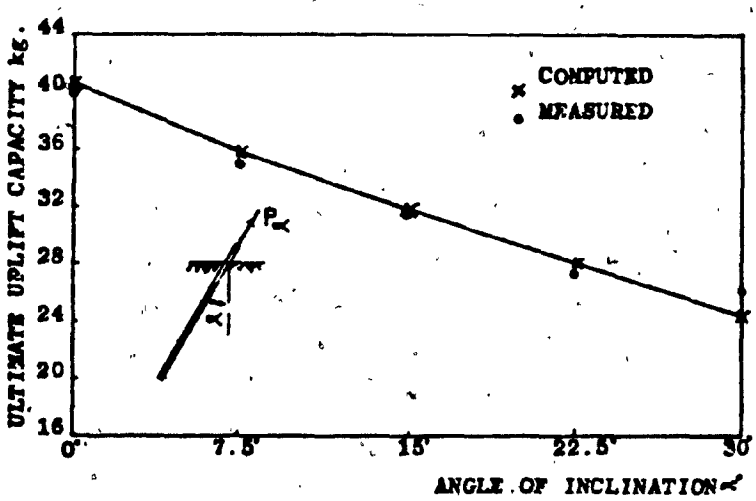


Fig. 2.5. Ultimate uplift capacity of vertical and inclined piles versus pile inclination

Using laboratory model tests on small footings (4" in diameter and 20" deep) in sand and field tests of cylindrical drilled piers (3.5 ft. in diameter and 21 ft. deep), Ismael & Klym (11) recommended that the coefficient of lateral earth pressure used in compression be equal to that used in uplift.

The ultimate uplift load being:

$$P_u = 1/2\ \gamma' L^2\ \pi B K_u \tan\phi' + W_p \qquad 2.7$$

in which: $\gamma'$ = effective unit weight of soil,

$K_u$ = coefficient of lateral earth pressure in uplift,

$\phi'$ = effective angle of shearing resistance.

The values of $K_u$ were in agreement with those suggested by Adams, Table (2.2), where N=No. of blows using Standard Penetration Test.

Summary of $K_u$ Values

| Soil description (1) | N value (2) | $K_u$ (3) |
|---|---|---|
| Very loose | 2-4 | 0.5 |
| Loose | 5-10 | 1.0 |
| Compact to dense | 11-50 | 1.5 |
| Very dense | > 50 | 2.0 |

Table 2.2

Load versus uplift is shown in Fig. (2.6) for the model test in loose sand.

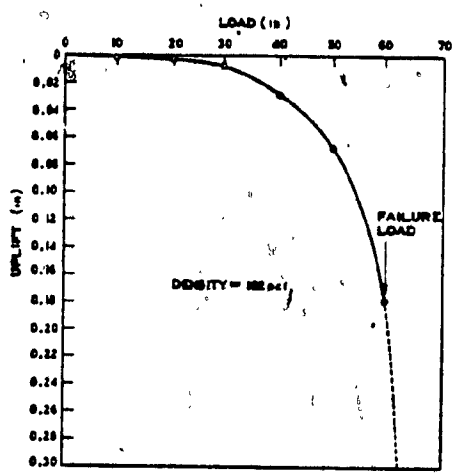


Fig. 2.6 - Load versus Uplift for Uplift Model Test in Loose Sand

Kulhaway et al.(13) performed a number of model tests to predict the uplift capacity of drilled shafts. Using the cylindrical shear method, Fig. (2.7), the uplift capacity is predicted by:

by: $$P_u = \overline{W} + \pi D \int_0^L K\gamma' Z \tan \phi' \, dz \qquad 2.8$$

where: K = lateral stress coefficient

Z = depth,

L = shaft length,

$\overline{W}$ = effective weight of shaft,

$\phi'$ = effective soil friction angle.

For a homogenous soil and linear stress increases the equation becomes: $p_u = \overline{W} + \pi D \frac{L^2}{2} K\gamma' \tan\phi'$ 2.9

A comparison of uplift capacity predictions shows that a good agreement is obtained with Ka in the loose tests, and $\sqrt{Kp}$ in the dense tests.

Ka and Kp, being respectively the active and passive earth pressure.

However, this hypothesis cannot be proven because the in-situ stresses and their variations were not measured and the fact that the dense test results correlated well with $\sqrt{Kp}$ is just considered to be fortuitous.

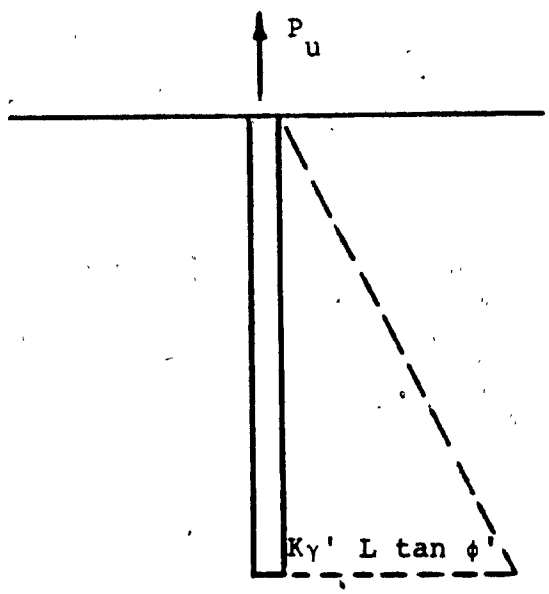


Fig. 2.7-Cylindrical Shear.

# CHAPTER III

# LABORATORY SET-UP AND PROPERTIES OF THE MATERIALS

## 3.1 General Description of The Experimental Set-Up

The experimental set-up used in the program is designed by Nguyen (18). It comprises a 4'x7'x7' deep steel frame test tank, designed for load tests on model test piles up to 5.5 feet long and 3 inches in diameter. The placement of sand in the test tank is carried out by depositing sand through a double slotted bottom distributing hopper installed on a carriage travelling back and forth over the test tank. Provisions are made to permit regulating the flow rate of sand, the speed of carriage travel and the height of fall of sand.

Once the tank is filled the model pile can be pushed into the sand deposit at various desired inclinations by a strain controlled screwjack attached to a loading column. After the completion of one test series in the tank, the sand will be transported to the storage tank (dimension 8'x8'x4') by means of a vacuum suction system. This same system is used to refill the test tank.

## 3.2 Testing Facilities

The main facility used in this experimental set-up consists of the sand distributing system, the sand conveying system and the loading equipment.

### 3.2.1 Sand Distributing System

The sand distributing system has been developed to provide a reliable means for preparing uniform sand beds. The main features of this system include a carriage and a distributing hopper.

#### a) Carriage

The carriage is chain driven on horizontal rails by an electronic controlled, variable speed 1/4 H.P.D.C. motor. The carriage is designed to run continuously on tracks over the 7 feet long test tank and reverse its direction by automatic photo electric switches installed at each end of the test tank. The accelerating and deccelerating to or from full travel speed is accomplished within 0.5 second. As a result of this short delay, a uniform sand deposit may be obtained within the central 6 feet of the sand

box. (Fig. 3.1 & Fig. 3.2).

b) Sand Distributing Hopper (Fig. 3.3)

The distributing hopper consists of a steel framed container (46.5" x 18" x 3.5"). The hopper bottom is provided with continuous double slots over its full length. The width of the slot can be adjusted by two bolts. A manual mechanism operated on springs and cables attached to an inverted steel angle is designed to provide a closing and opening gate for the double slots. The sand distributing hopper can be raised up or lowered down vertically into the test tank by a hand operated winch, (Fig. 3.2). The hopper may be secured at desired elevations by means of pins and holes drilled at 3 inches spacings on the guiding frame, which is bolted onto the chassis of the carriage.

### 3.2.2 Sand Conveying System

The sand conveying system is designed to satisfy two basic requirements: to transport sand from ground level to the storage bin located on top of the loading frame and to empty the sand box after each test series.

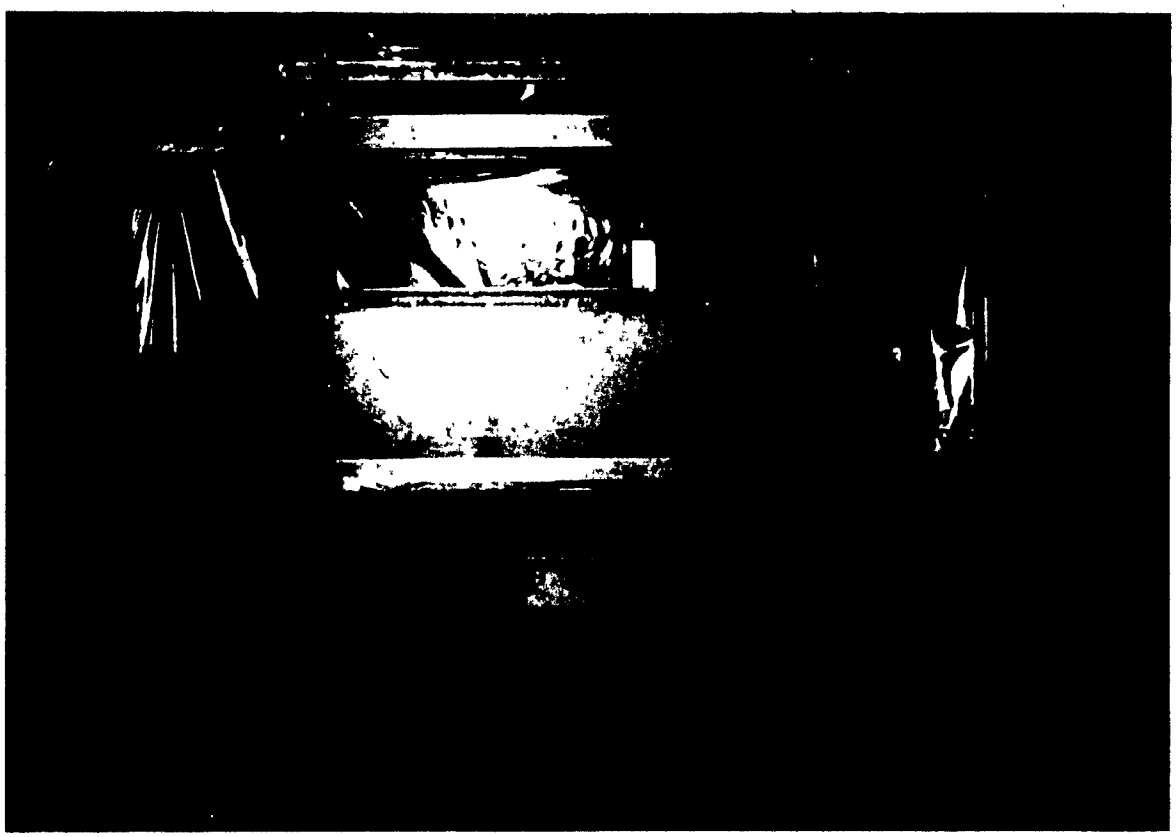

Figure 3.1 Carriage running on tracks (Front view).

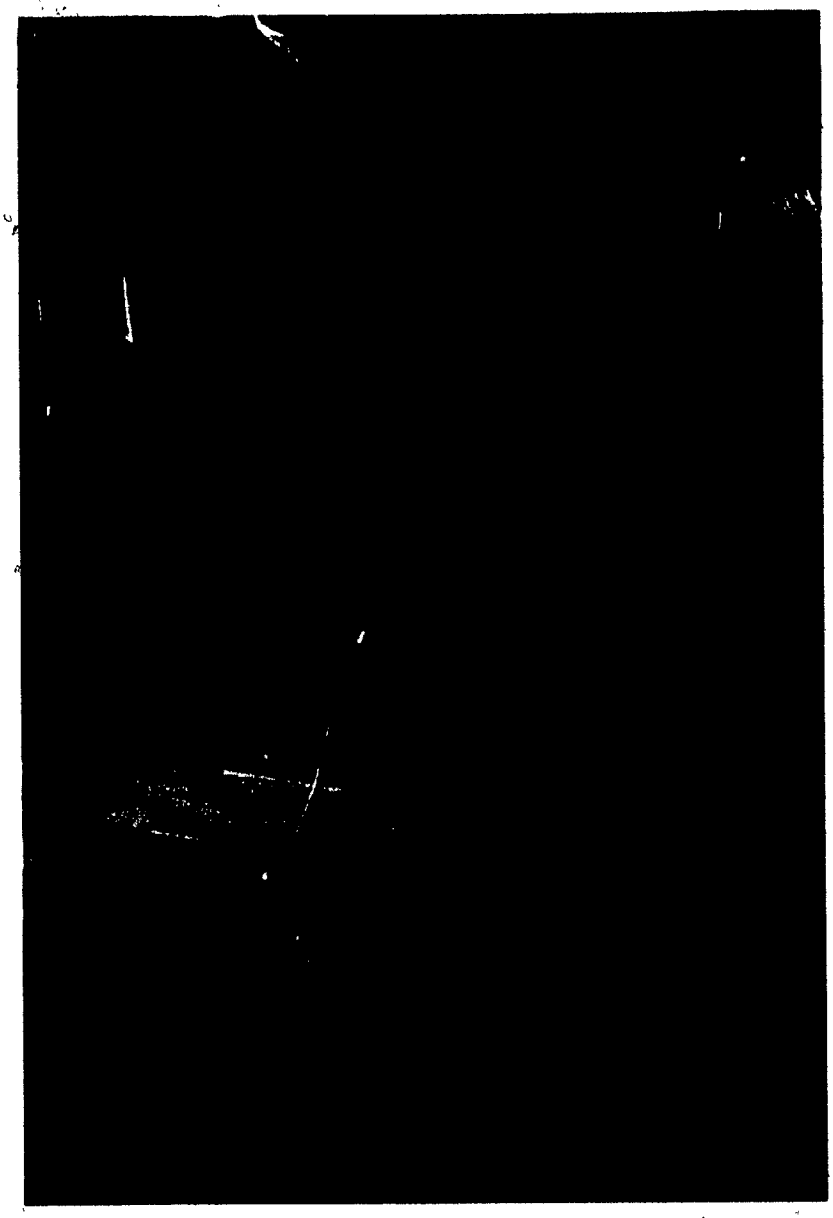

Figure 3.2 Carriage running on tracks
(rear view)

Figure 3.3 Close-up of the sand distributing hopper in action

This system consists of a 10 H.P. vacuum pump (Fig. 3.4), a storage bin and separator auxiliary tank (Fig. 3.5), and a pick-up tool (Fig. 3.6), connected by 2.5 inch diameter flexible hoses. The general arrangement of the system is shown in Fig. (3.7).

### 3.2.3 Loading Equipment

The loading equipment includes a motorized 15 ton capacity screw jack with 3 feet maximum travel, mounted on a steel plate which is bolted onto a (4"x5"x5/16") loading column steel tubing. This set-up allows pulling of model piles vertically or at any angle up to $45^{\circ}$ with the vertical by a system of a sleeve, a pin and supporting frames. The combination of a gear shift, a gear reducer and an electronic speed-controlled device (Fig. 3.8) provide the screw jack with a loading and unloading speed varying from 0.01" per minute to 1.0" per minute.

## 3.3 Model Piles

Two model piles are used in this investigation. The surface of both pile shafts is covered with sand paper to assure roughness and hence, larger magnitudes of skin friction measurements.

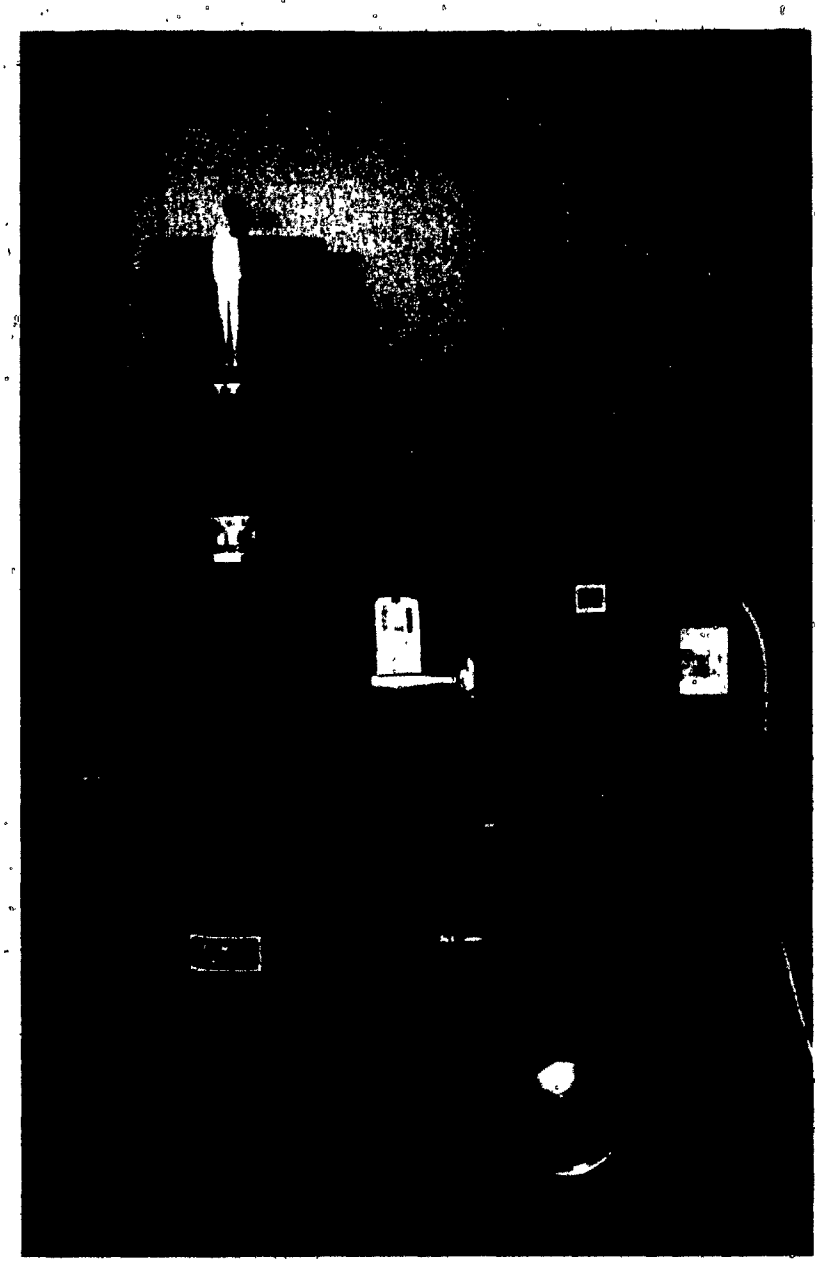

Figure 3.4: 10 H.P. vaccum pump

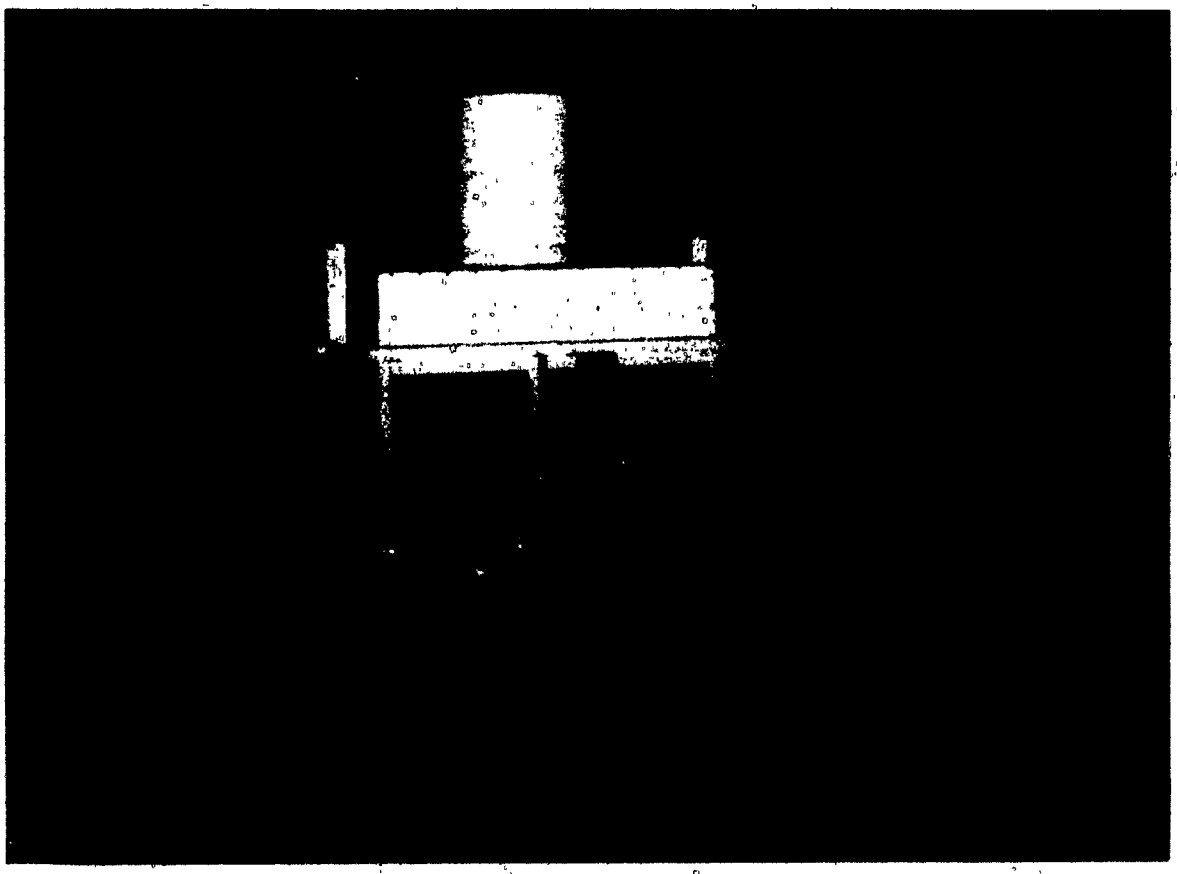

Figure 3.5: Storage bin & separator auxiliary tank

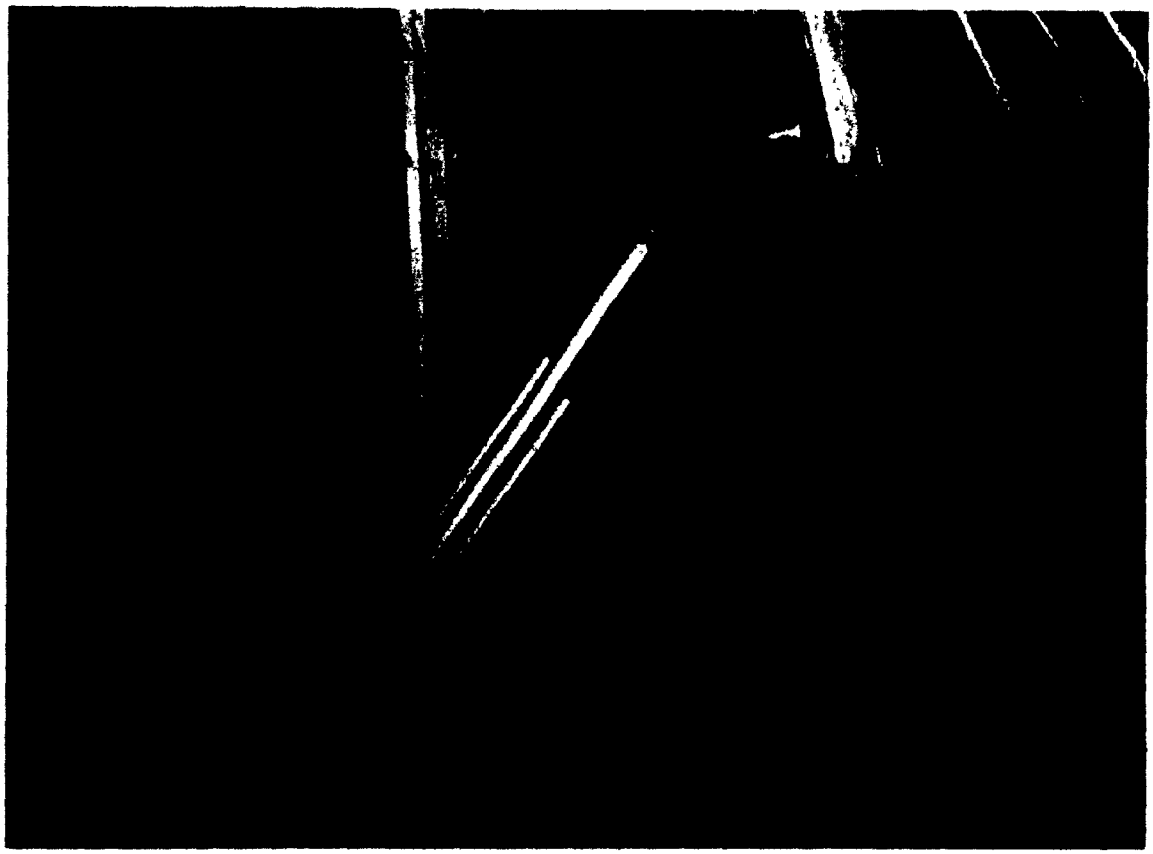

Figure 3.6: Pick-up tool

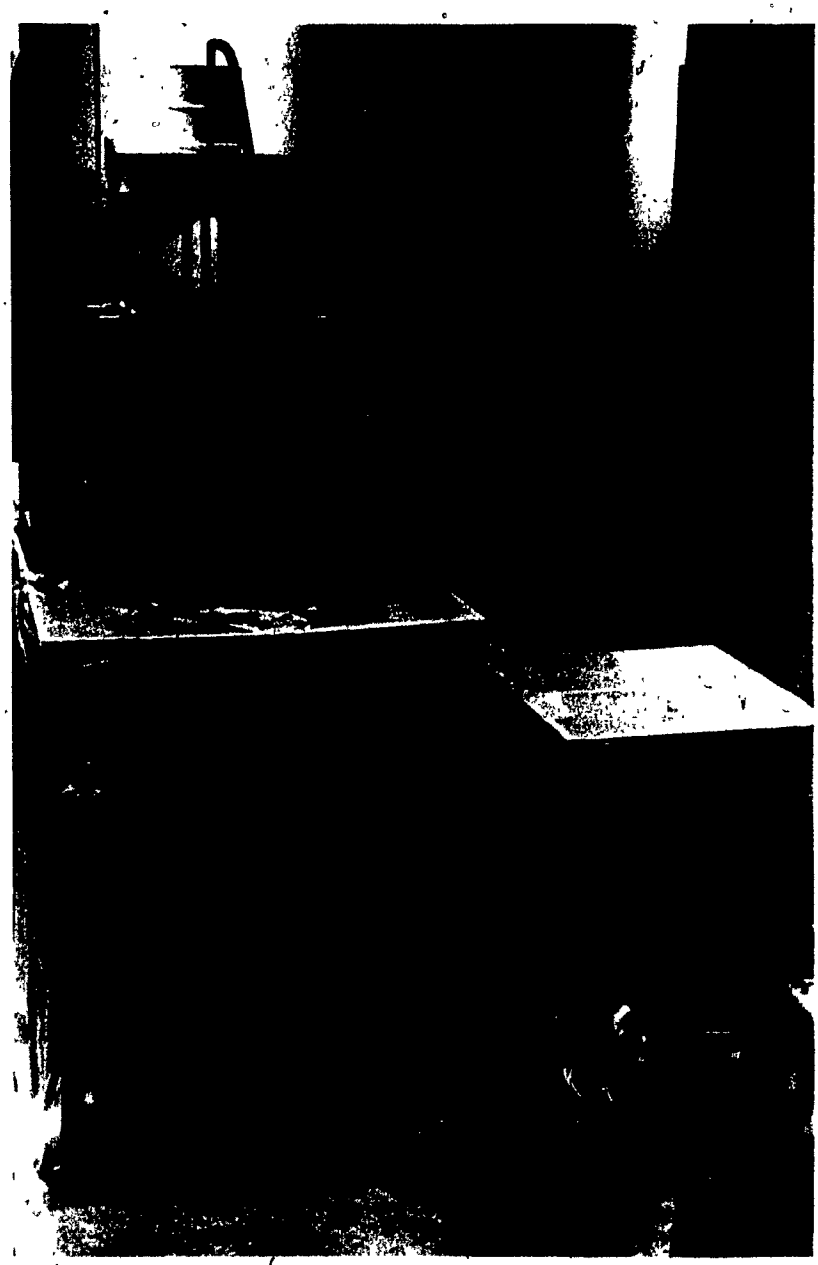

Figure 3.7 General arrangement of the sand conveying system

Figure 3.8 Loading equipment

### 3.3.1 Model Pile 1

The model pile 1 is a steel pipe 66 inches long and 1.50 inch outside diameter. At the pile top, a proving ring is installed between the loading pile cap and the screwjack. This arrangement allows the evaluation of the skin friction over the embedded pile length.

### 3.3.2 Pile Cap Design For Model Pile 1

A special cap is designed for model pile 1 to be able to hook it to the proving ring which is attached to the screwjack. (Fig. 3.9) shows the details of this cap.

### 3.3.3 Model Pile 2

Model pile 2 consists of steel and aluminum pipe sections (3 inches outside diameter) connected to a total length of 66 inches. A load cell is installed at the pile top to measure the total pull-out load applied.

### 3.3.4 Pile Cap Design For Model Pile 2

A special cap is designed for model pile 2 to be

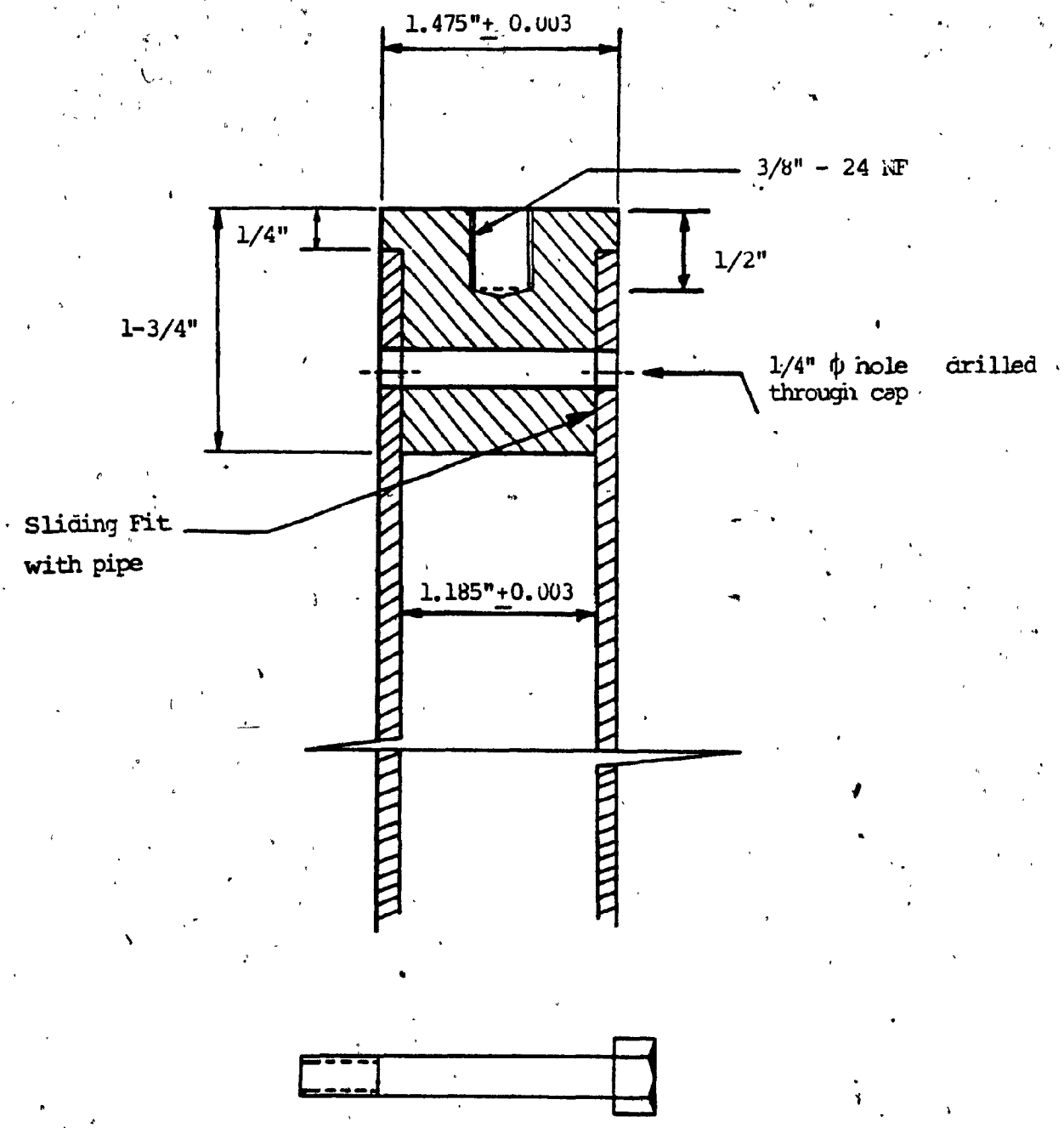


Figure 3.9 Pile cap design for model pile 1.

able to hook it to the load cell which is attached to the screwjack. (Fig.'s 3.10 through 3.15) show the details of this arrangement.

## 3.4 Materials Used

The sand used in this investigation is called "Morie Sand" and is imported from U.S.A.

## 3.5 Mechanical Properties

### 3.5.1 Grain Size Distribution

The grain size distribution indicated a medium, uniform sand (See Table 3.1).

GRAIN SIZE DISTRIBUTION

| Sieve Size (U.S. Standard) | % Passing |
|---|---|
| 10 | 100 |
| 16 | 60.1 |
| 20 | 11.8 |
| 30 | 1.7 |
| 50 | 0.2 |
| 100 | 0. |

Table 3.1

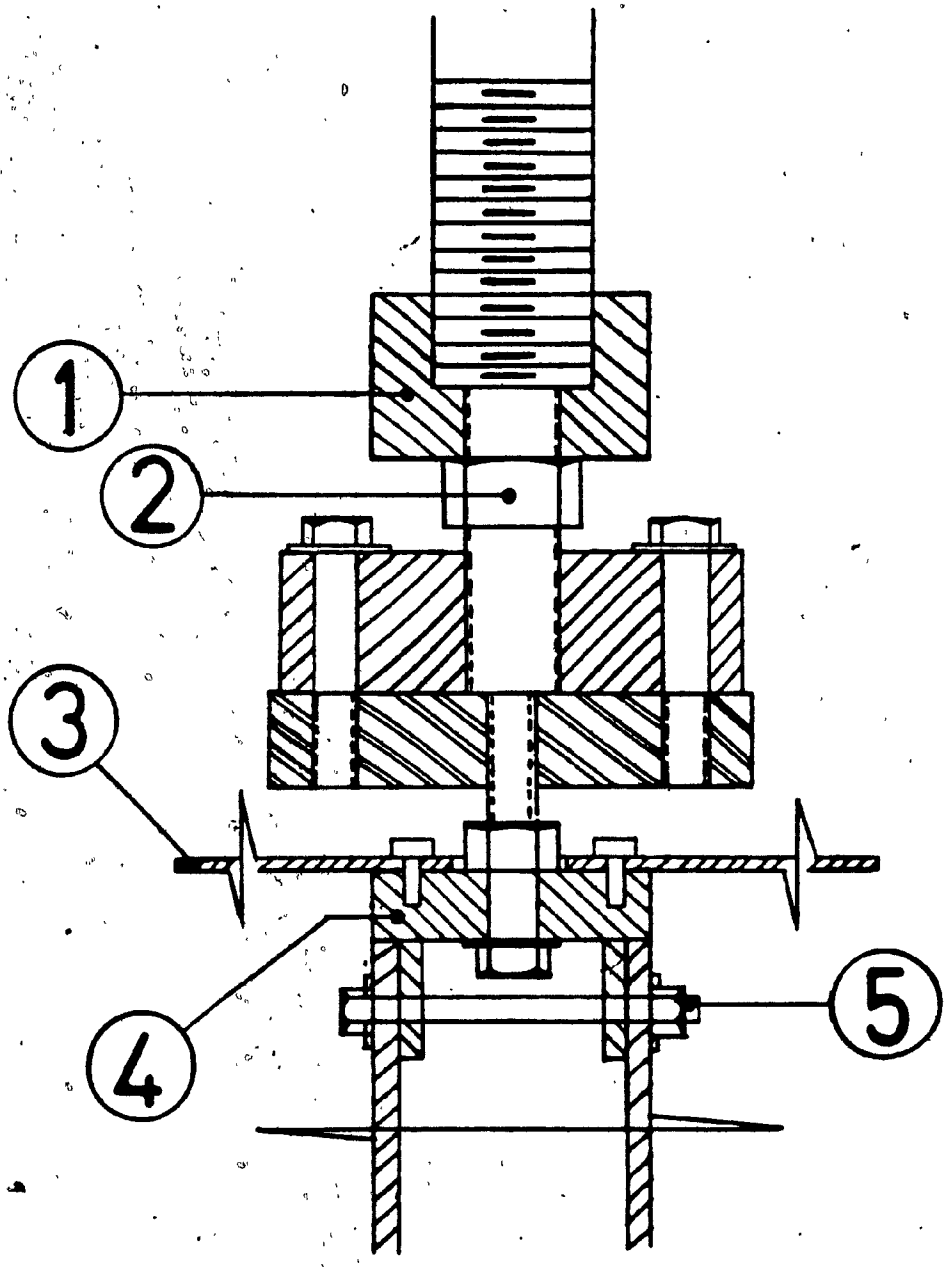


Fig. 3.10: Arrangement of pile cap load cell and screw jack

COMPONENT (1)

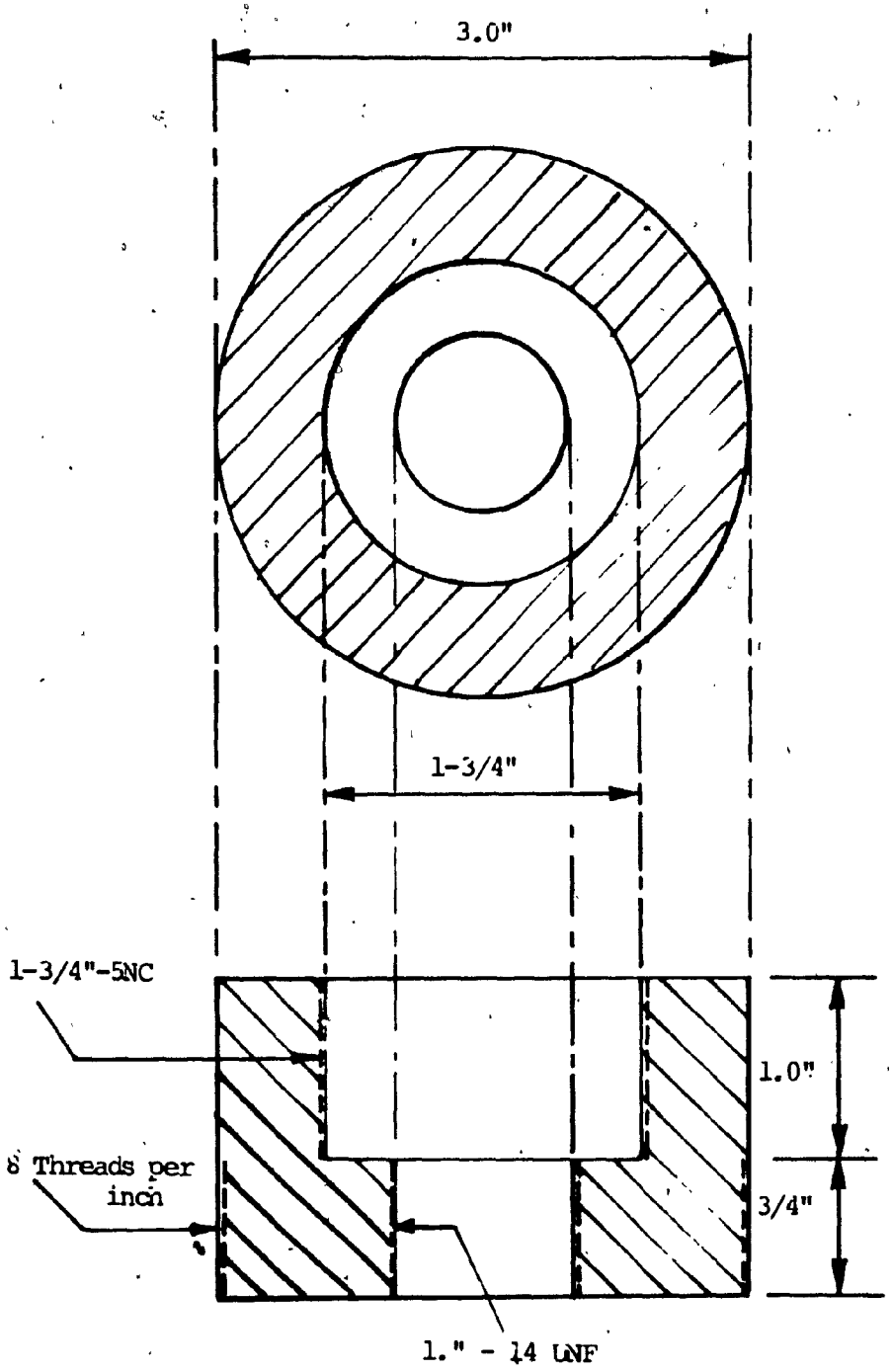


Figure 3.11 - Special Cap to the Screw-Jack

COMPONENT (2)

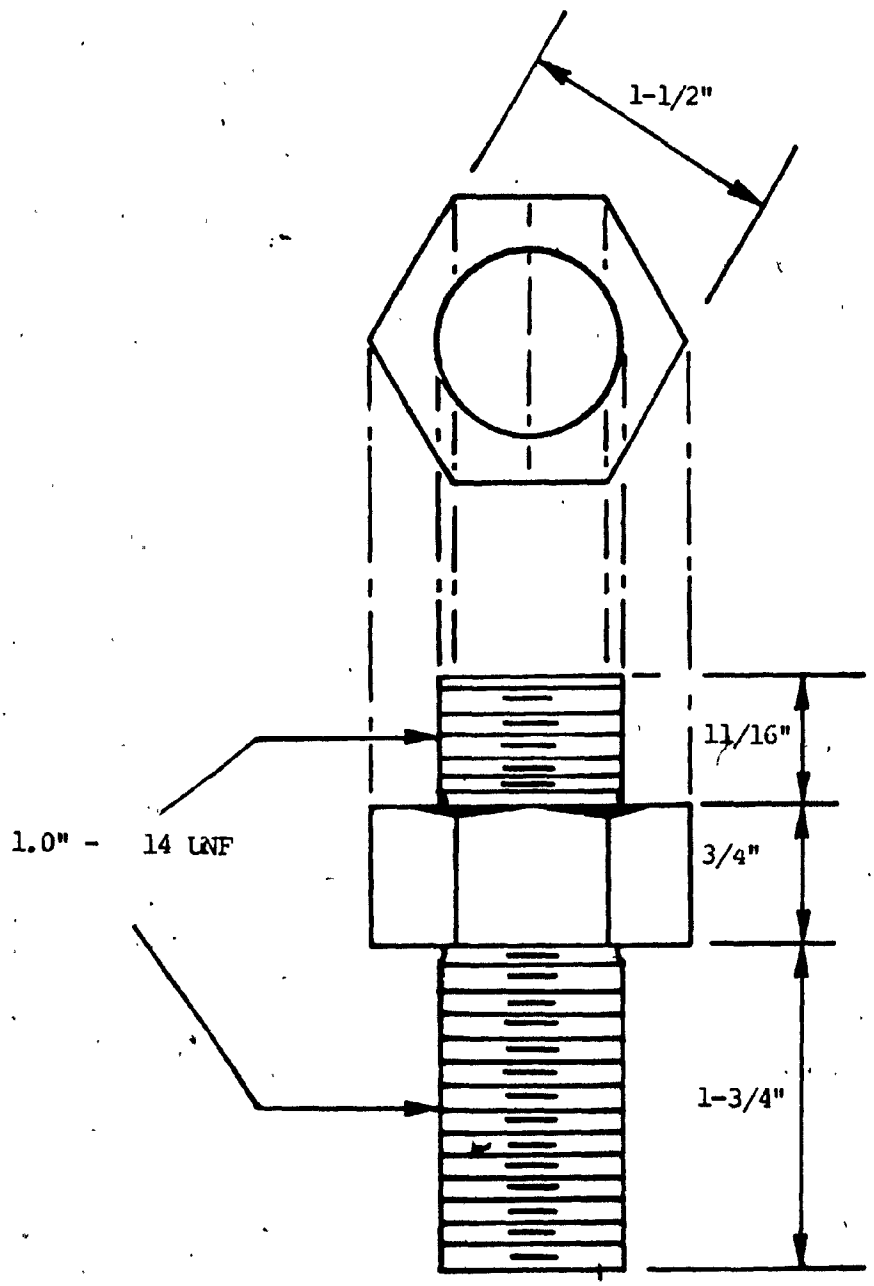


Figure 3.12 - Screw Connecting Load Cell to Cap of Screw-Jack

COMPONENT (3)

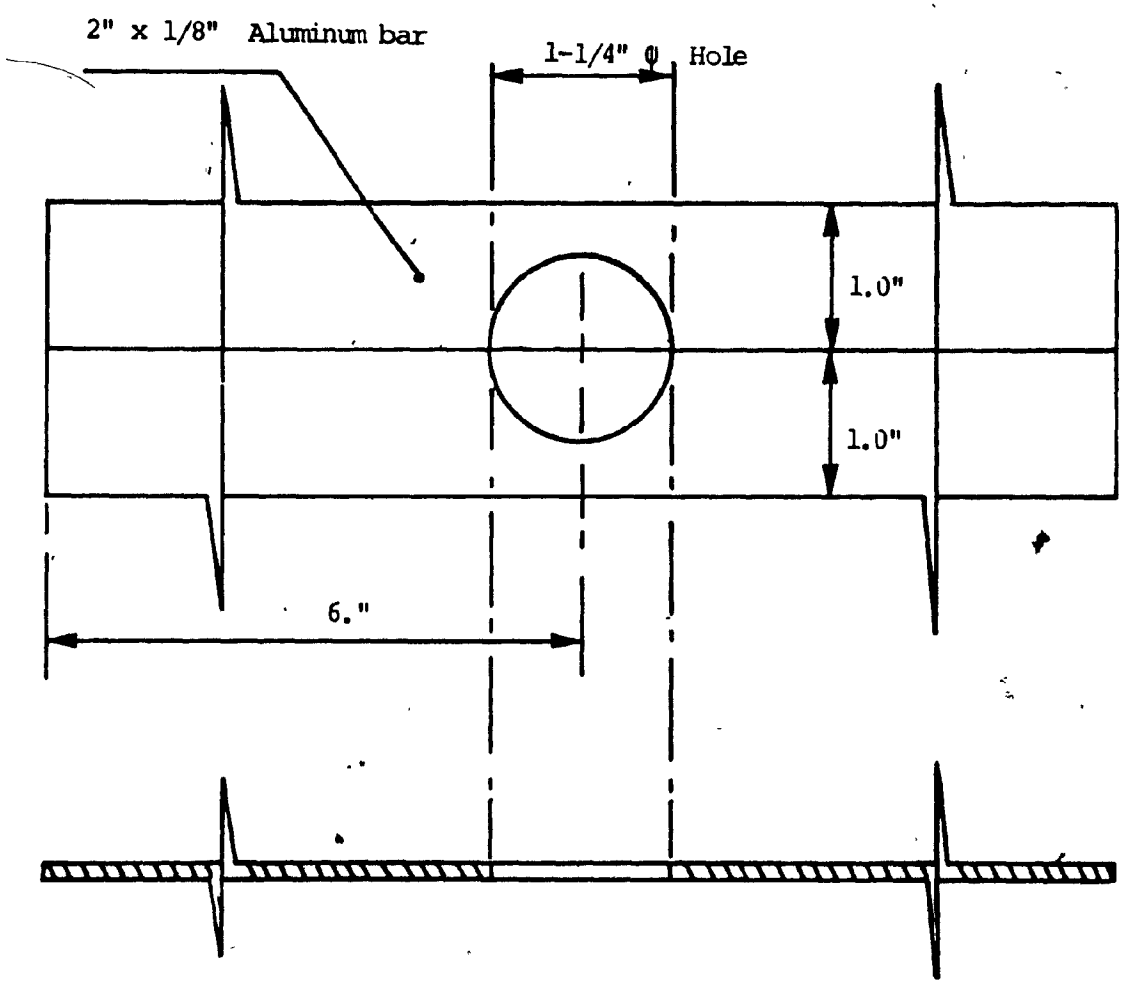


Figure 3.13 Aluminum Bar for Dial Gages

COMPONENT (4)

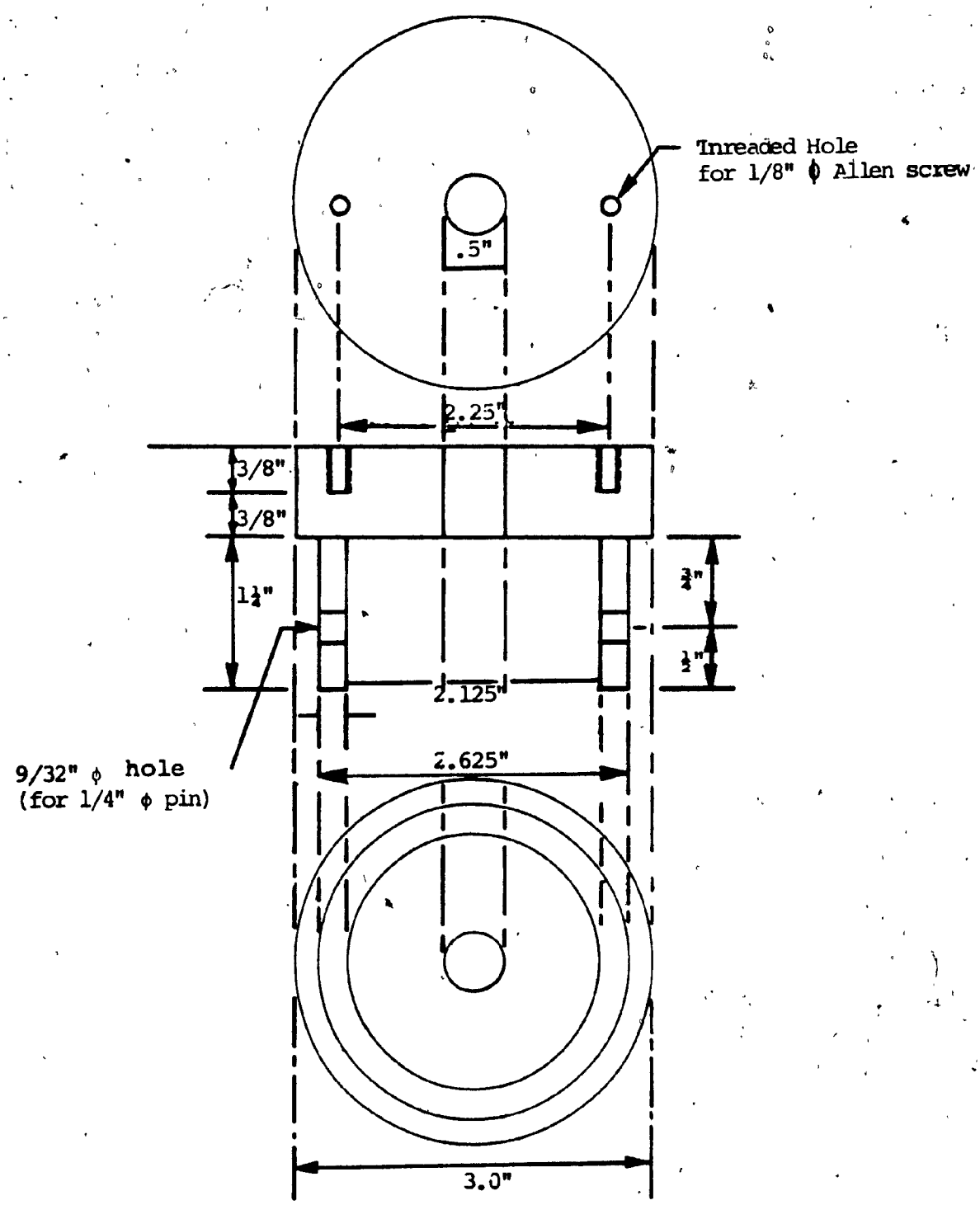


Figure 3.14 - Pile Cap

COMPONENT (5)

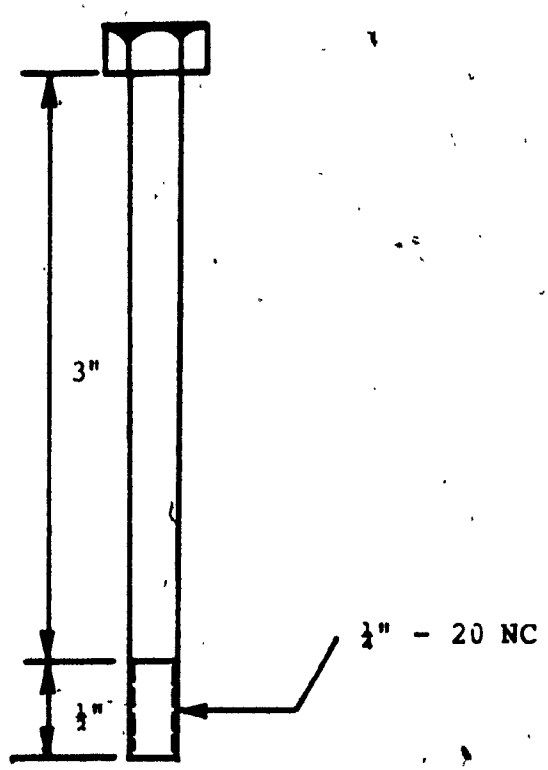


Figure 3.15 - Pin Holding Pile to Cap

$D_{10} = 0.82$ mm

$D_{60} = 1.19$ mm

Coefficient of Uniformity: $C_u = \frac{D_{60}}{D_{10}} = \frac{1.19}{0.82} = 1.45$

### 3.5.2 Specific Gravity Test

Several Tests are conducted as seen in Table 3.2 and the average value of the specific gravity is calculated and used.

SPECIFIC GRAVITY TEST

| Test No. | Wt of Beaker & Water (grams) | Wt of Sand (grams) | Wt of Sand +Beaker & Water (grams) | Temperature (°C) | $G_s$ |
|---|---|---|---|---|---|
| 1 | 654 | 150 | 747.6 | 25 | 2.656 |
| 2 | 654 | 150 | 747.8 | 23 | 2.667 |
| 3 | 676.5 | 150 | 770.3 | 26 | 2.665 |
| 4 | 654 | 150 | 747.7 | 25 | 2.661 |

Table 3.2

The average value of $G_s = \frac{2.656 + 2.667 + 2.665 + 2.661}{4} = 2.662$

### 3.5.3 Maximum And Minimum Densities

Maximum and minimum densities of this sand as determined by standard Procedures (ASTM D2049) are calculated and average values are shown in Table 3.3, with a Standard deviation of 0.625.

MAXIMUM & MINIMUM DENSITIES

| Density | Dry Unit Weight (P.C.F.) | Void Ratio | Porosity % |
|---|---|---|---|
| Maximum | 104.5 | 0.590 | 37.1 |
| Minimum | 91.5 | 0.815 | 44.9 |

Table 3.3

### 3.5.4 Direct Shear Test Results (Sand/Sand)

A series of direct shear tests are performed with nominal normal stresses $\sigma_n$ = 5, 10, 40 and 80 psi.

The nominal relative densities of sand for

each of the stresses are: 30%, 50%, 70% and 90%.

A 1.5% error in the value of e is allowed.

Using $R.D. = \frac{e_{max} - e}{e_{max} - e_{min}}$ with $e_{max} = 0.815$ and $e_{min} = 0.590$

| | 1.5% Error (Allowable) |
|---|---|
| R.D. = 30% → e = 0.747 | 0.736 < e < 0.759 |
| R.D. = 50% → e = 0.703 | 0.692 < e < 0.713 |
| R.D. = 70% → e = 0.658 | 0.648 < e < 0.668 |
| R.D. = 90% → e = 0.613 | 0.604 < e < 0.622 |

Table 3.4 summarizes the results of the direct shear tests and figure 3.16 graphs the results to determine the angle of internal friction of sand for different relative densities.

### 3.5.5 Direct Shear Test Results (Sand/Sandpaper)

To determine the angle of internal friction between sand and sandpaper, a steel block with sandpaper glued on its top replaces the sand in the lower part of the shear box (19). The tests are performed with the same nominal stresses and relative densities & with the same 1.5% error allowed as those for Sand/Sand tests.

Table 3.5 summarizes the results of these tests and figure 3.17 graphs results to determine the angle of internal friction between sand and sandpaper for different relative densities.

### 3.5.6 Triaxial Test Results

A series of triaxial tests are performed on the Morie sand under various states of packing and cell pressures. Using a sample size of 1.5" diameter, Cell pressures of 5, 10, 20 & 40 psi and void ratios of 0.775 , 0.724 & 0.672, the results are tabulated in Table 3.6. Figures 3.18 through 3.20 graph the results of the test indicating the values of the angle of internal friction for different relative densities.

Figure 3.21 shows the results of all tests on the same graph for the sake of comparison.

## 3.6 Calibration of The Unit Weight of Sand

The ability to obtain an accurate estimate of the density of a soil is of critical importance. Without such data the relationship between density and angle of internal friction, $\phi$ cannot be achieved. It was imperative

| Nominal Relative Density (%) | NOMINAL NORMAL STRESS, $\sigma_n$ (psi) | | | | | | | | | | | |
|---|---|---|---|---|---|---|---|---|---|---|---|---|
| | 5 | | | 10 | | | 40 | | | 80 | | |
| | e | $\sigma_n$ (psi) | $\tau_{max}$ (psi) | e | $\sigma_n$ (psi) | $\tau_{max}$ (psi) | e | $\sigma_n$ (psi) | $\tau_{max}$ (psi) | e | $\sigma_n$ (psi) | $\tau_{max}$ (psi) |
| 30 | 0.755 | 4.97 | 4.16 | 0.755 | 10.145 | 8.10 | 0.755 | 40.145 | 30.92 | 0.755 | 80.17 | 60.99 |
| 50 | 0.705 | 4.97 | 4.48 | 0.705 | 10.145 | 8.32 | 0.705 | 40.145 | 33.06 | 0.705 | 80.17 | 65.3 |
| 70 | 0.653 | 4.97 | 5.12 | 0.653 | 10.145 | 9.17 | 0.653 | 40.145 | 36.5 | 0.653 | 80.17 | 72.09 |
| 90 | 0.613 | 4.97 | 6.61 | 0.613 | 10.145 | 10.03 | 0.617 | 40.145 | 39.2 | 0.613 | 80.17 | 78.5 |

Table 3.4 Summary of Direct Shear Test Results (Sand/Sand).

| Nominal Relative Density (%) | NOMINAL NORMAL STRESS, $\sigma_n$ (psi) | | | | | | | | | | | |
|---|---|---|---|---|---|---|---|---|---|---|---|---|
| | 5 | | | 10 | | | 40 | | | 80 | | |
| | e | $\sigma_n$(psi) | $\tau_{max}$(psi) | e | $\sigma_n$(psi) | $\tau_{max}$(psi) | e | $\sigma_n$(psi) | $\tau_{max}$(psi) | e | $\sigma_n$(psi) | $\tau_{max}$(psi) |
| 30 | 0.740 | 4.97 | 4.26 | 0.740 | 10.145 | 8.32 | 0.740 | 40.145 | 31.35 | 0.740 | 80.17 | 62.28 |
| 50 | 0.700 | 4.97 | 4.69 | 0.700 | 10.145 | 8.74 | 0.700 | 40.145 | 34.12 | 0.700 | 80.17 | 67.82 |
| 70 | 0.661 | 4.97 | 5.12 | 0.661 | 10.145 | 9.38 | 0.661 | 40.145 | 37.32 | 0.661 | 80.17 | 74.22 |
| 90 | 0.606 | 4.97 | 6.4 | 0.606 | 10.145 | 10.45 | 0.606 | 40.145 | 42.01 | 0.606 | 80.17 | 80.62 |

Table 3.5: Summary of Direct Shear Test Result (Sand/Sand Paper).

## TRIAXIAL TEST RESULTS

| | Relative Density = 17.8% | | | | Relative Density = 40.7% | | | | Relative Density = 63.6% | | | |
|---|---|---|---|---|---|---|---|---|---|---|---|---|
| Cell Pressure | 5 | 10 | 20 | 40 | 5 | 10 | 20 | 40 | 5 | 10 | 20 | 40 |
| Dial Pressure | 33.75 | 58.33 | 99.74 | 191.08 | 41.29 | 62.18 | 107.31 | 198.72 | 42.84 | 70.51 | 113.42 | 216.56 |
| $\sigma_1 - \sigma_3 = P/A'$ | 17.51 | 30.74 | 52.73 | 101.94 | 19.7 | 32.97 | 58.7 | 108.59 | 22.85 | 38.07 | 63.35 | 117.98 |
| $\sigma_1$ | 22.51 | 40.74 | 72.73 | 141.94 | 24.7 | 42.97 | 78.7 | 148.59 | 27.85 | 48.07 | 82.35 | 157.98 |

Table 3.6

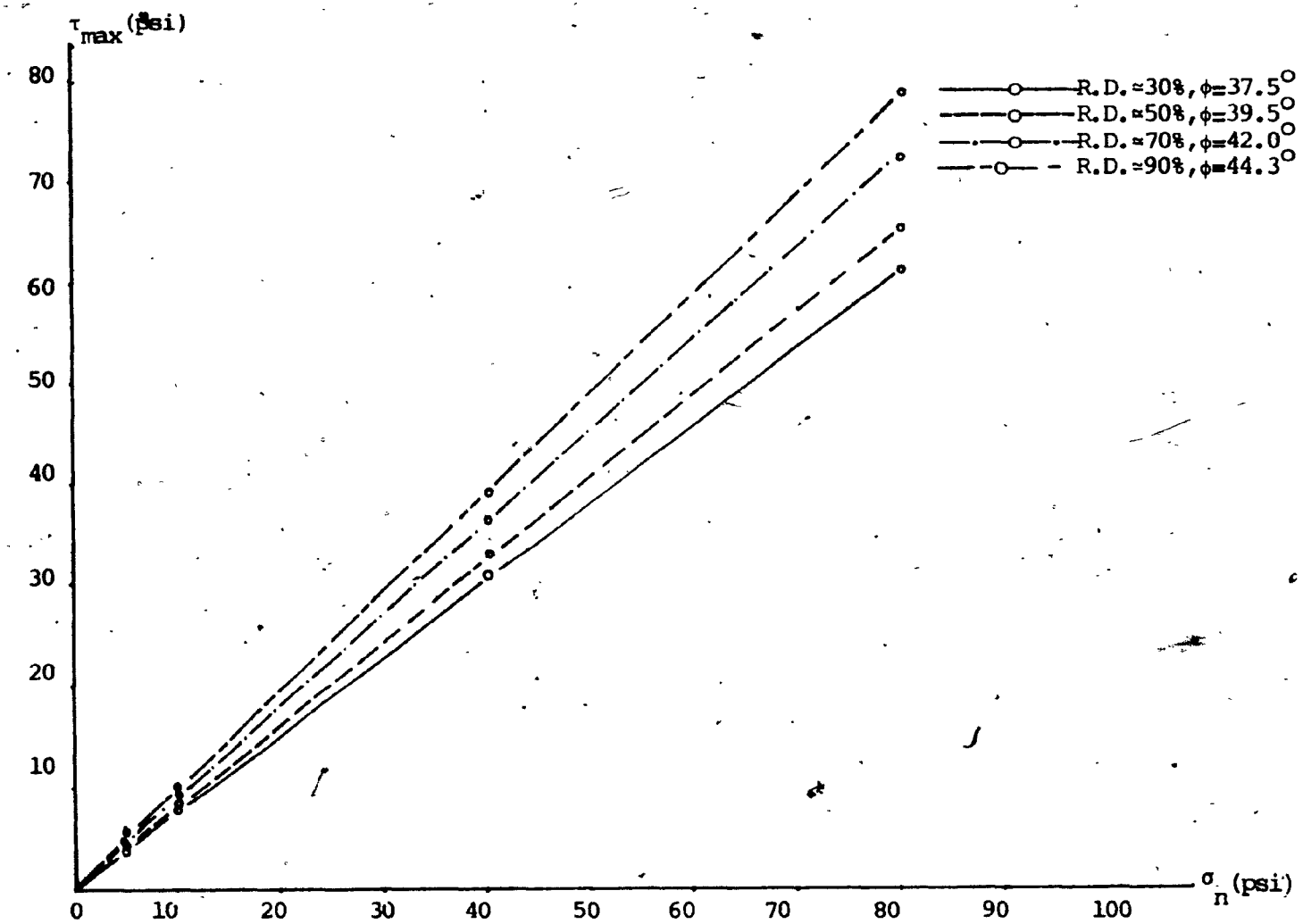


Fig. 3.16: Direct Shear Test Results (Sand/Sand)

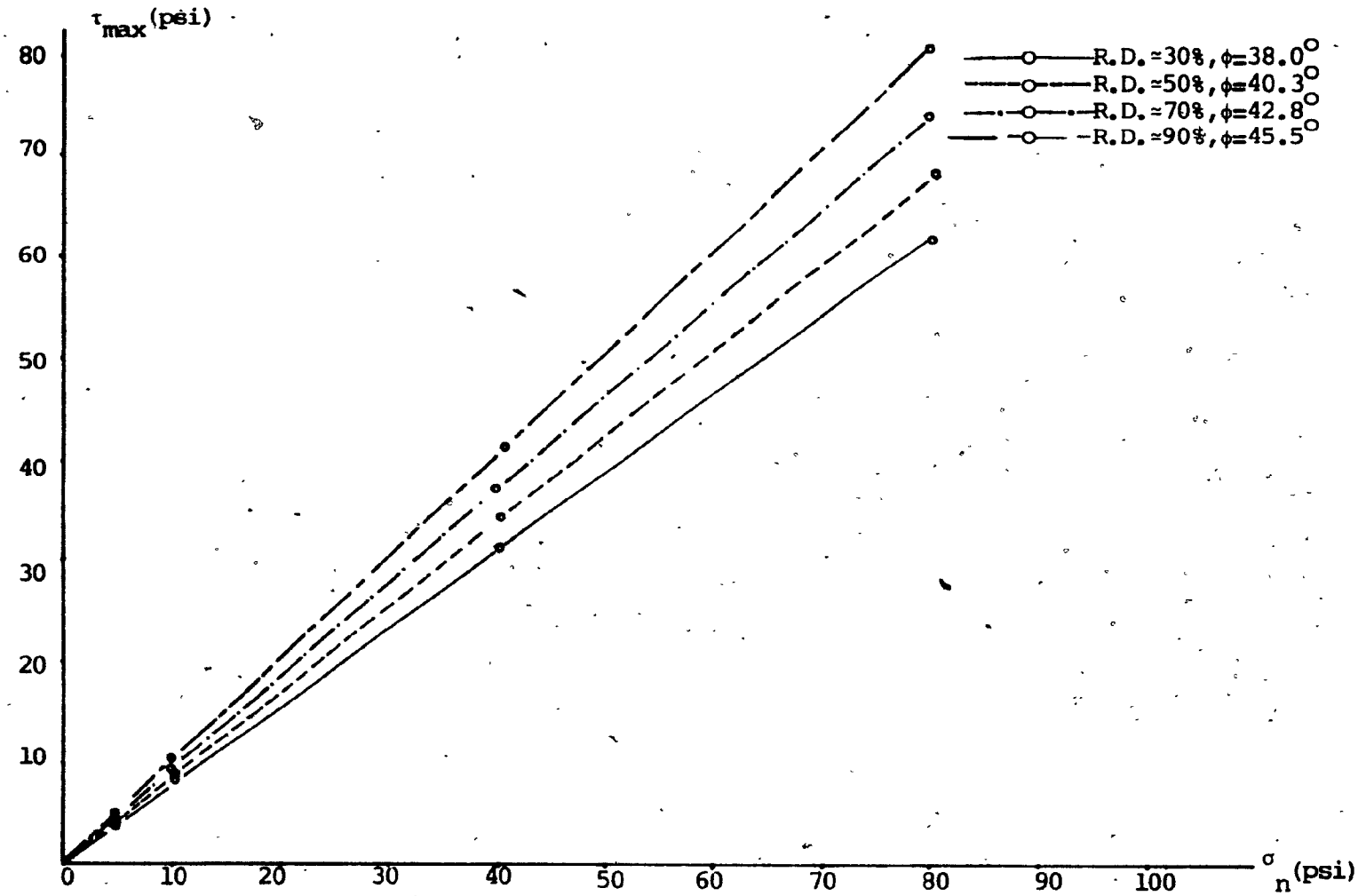


Fig. 3.17: Direct Shear Test Results (Sand/Sand Paper)

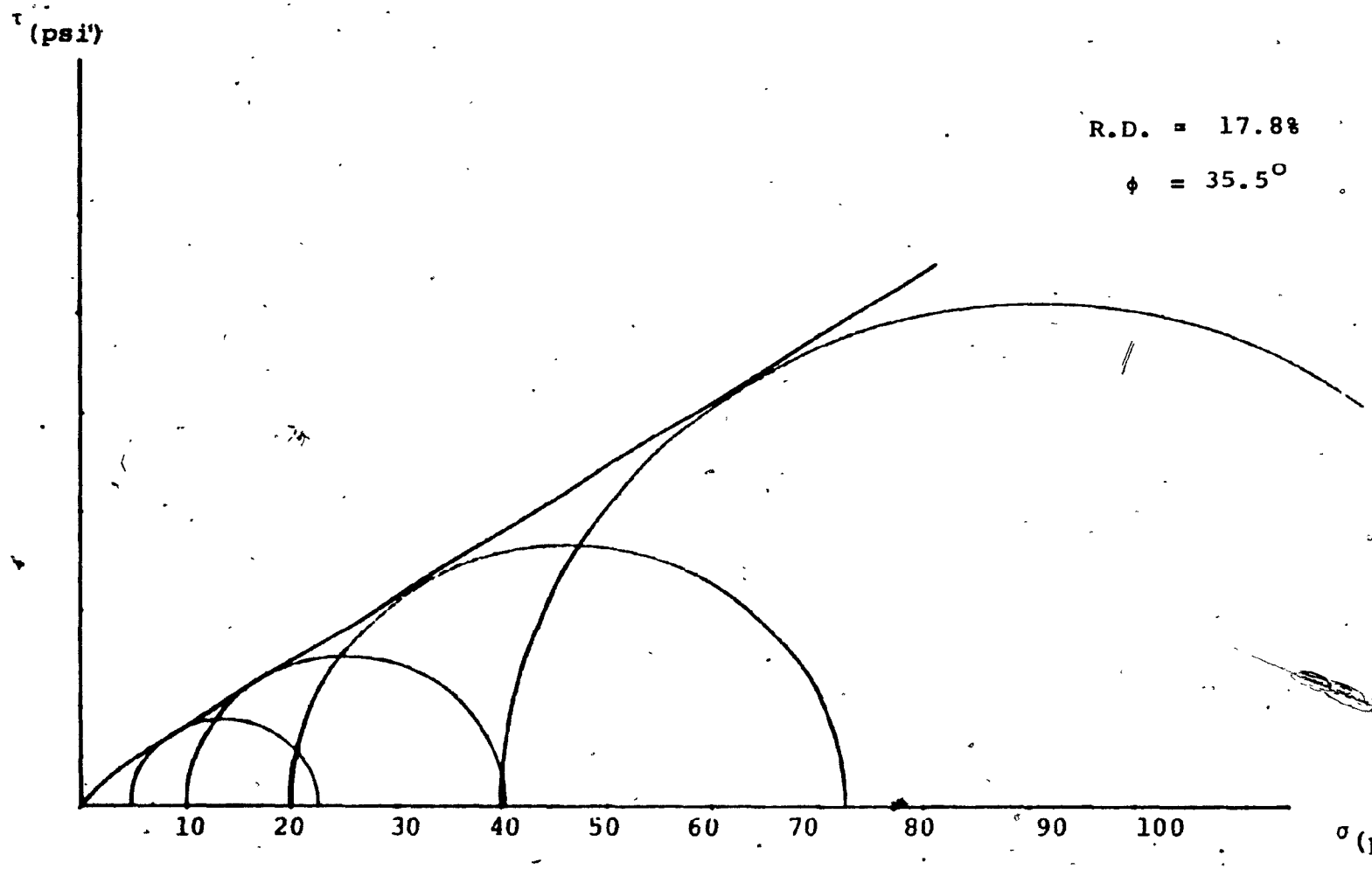


Fig. 3.18: Triaxial Test Results For a R.D. = 17.8%

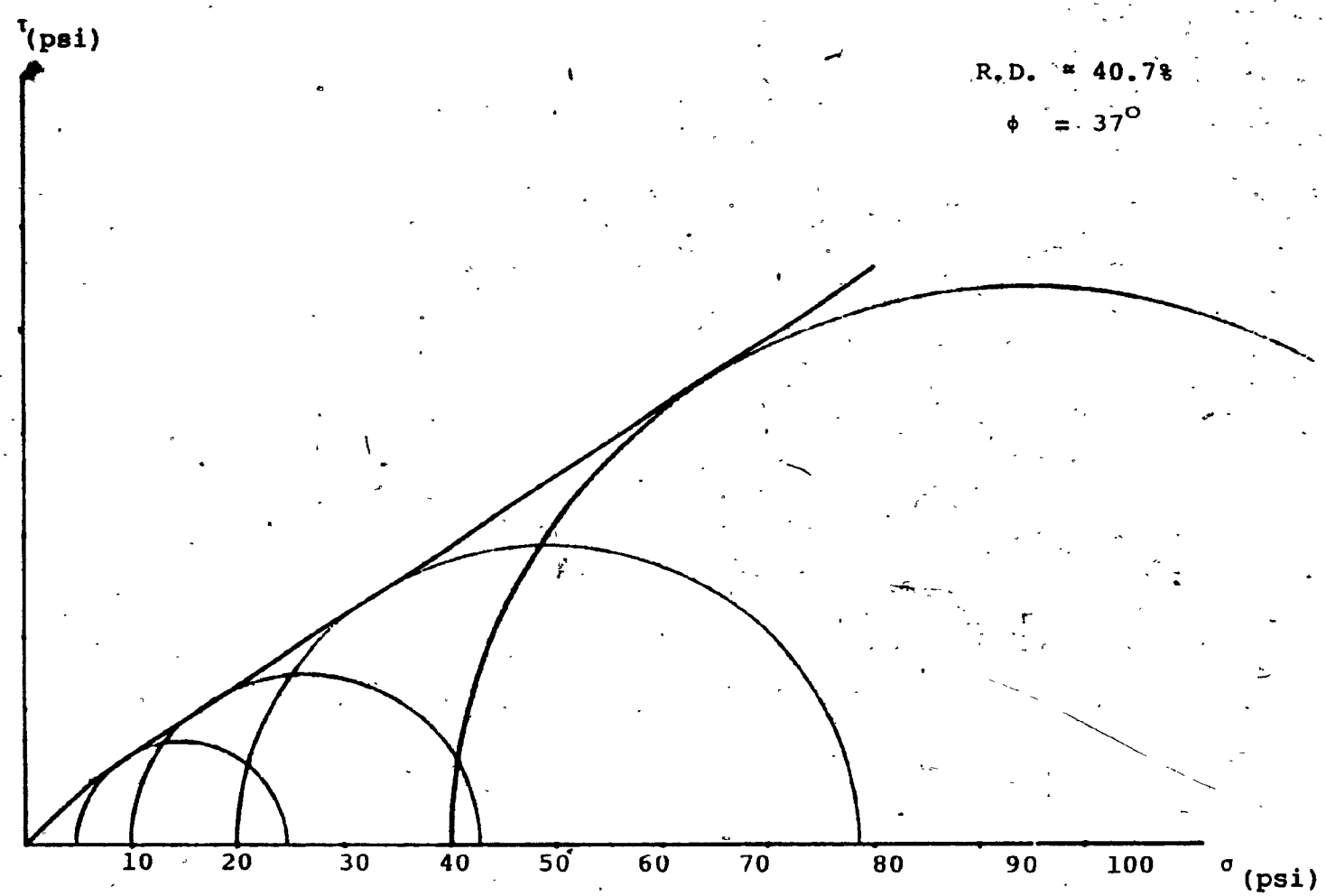


Fig. 3.19: Triaxial Test Results For a R.D. = 40.7%

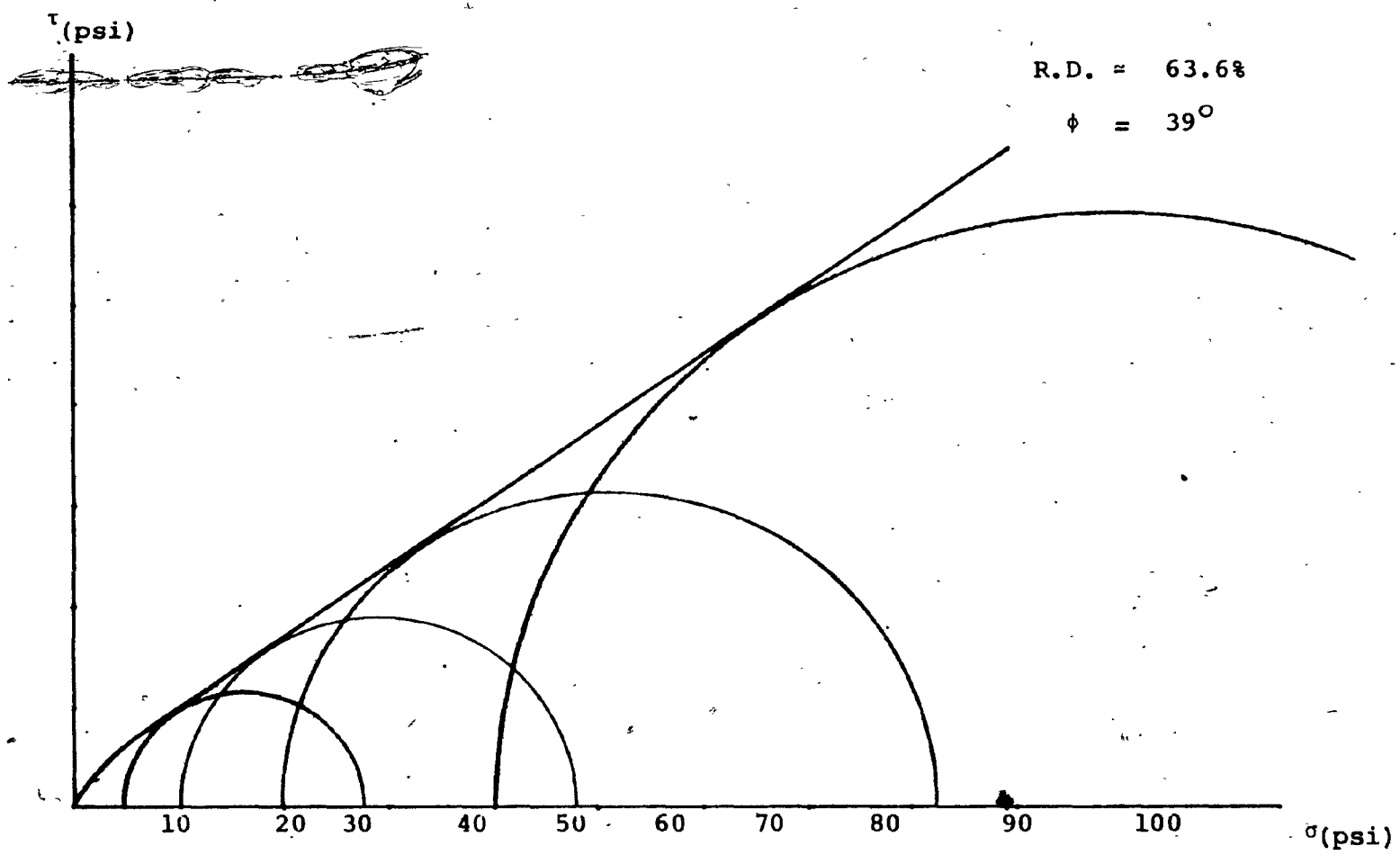


Fig. 3.20: Triaxial Test Results for a R.D. ≈ 63.6%

that the correct density of the deposit be established for the results to have any significance. Such a measure could be obtained by calibrating the height of fall of the sand to density, and with the use of density pots.

### 3.6.1 Density Pots

The density pot provided an excellent means of obtaining the density at any location in the test pit. 23 pots of known weights and volumes are placed on a levelled surface of sand, Fig. 3.22. Several heights of fall of sand are tried. After each test, the pots are carefully removed and the excess sand is scraped off, then each pot is weighed and the density is calculated.

### 3.6.2 Relative Density vs. Ht of Drop

Using the equations

$$e = \frac{G\gamma_\omega}{\gamma_d} - 1 \quad \& \quad R.D. = \frac{e_{max} - e}{e_{max} - e_{min}}$$

and knowing that;

$$G = 2.662, \quad e_{max} = 0.815 \quad \& \quad e_{min} = 0.590$$

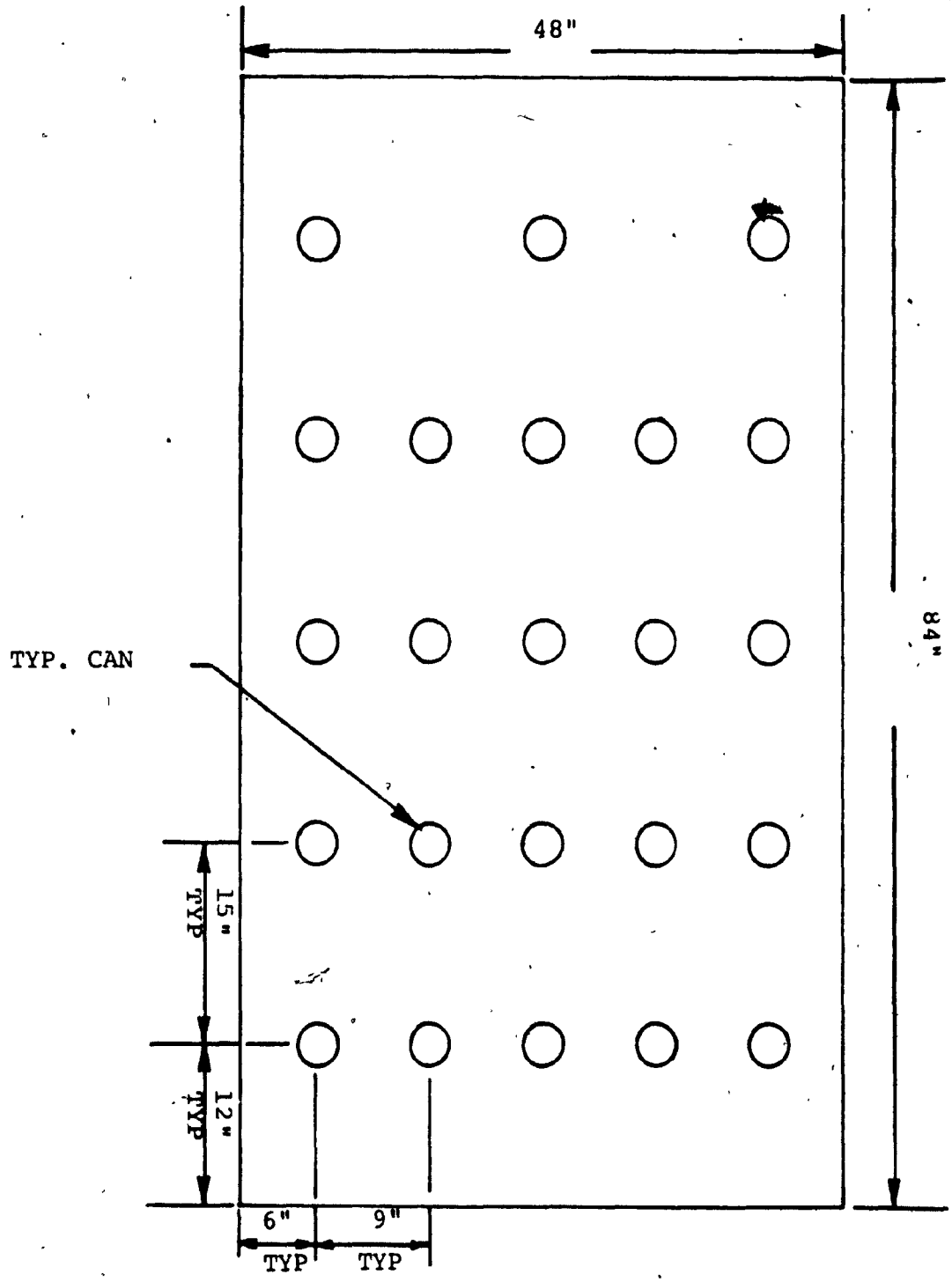


Fig.3.22 - Density Pot Placement.

Table 3.7 is established, with average values of $\gamma_d$ (g/cm$^3$) and a standard deviation of 0.013.

The calibration curve of the height of drop vs. $\gamma_d$ is shown on Fig. 3.23

Table 3.7

Values of dry unit weight, void ratio & relative density vs. Ht of Drop

| Height (in) | $\gamma_d$ (g/cm$^3$) | $\gamma_d$ (lb/ft$^3$) | e | R.D. | R.D.% |
|---|---|---|---|---|---|
| 6 | 1.560 | 97.34 | 0.706 | 0.483 | 48.3 |
| 12 | 1.582 | 98.72 | 0.683 | 0.589 | 58.9 |
| 18 | 1.589 | 99.15 | 0.675 | 0.622 | 62.2 |
| 24 | 1.594 | 99.47 | 0.670 | 0.645 | 64.5 |
| 30 | 1.595 | 99.53 | 0.669 | 0.650 | 65.0 |
| 44 | 1.596 | 99.59 | 0.668 | 0.655 | 65.5 |
| 56 | 1.596 | 99.59 | 0.668 | 0.655 | 65.5 |

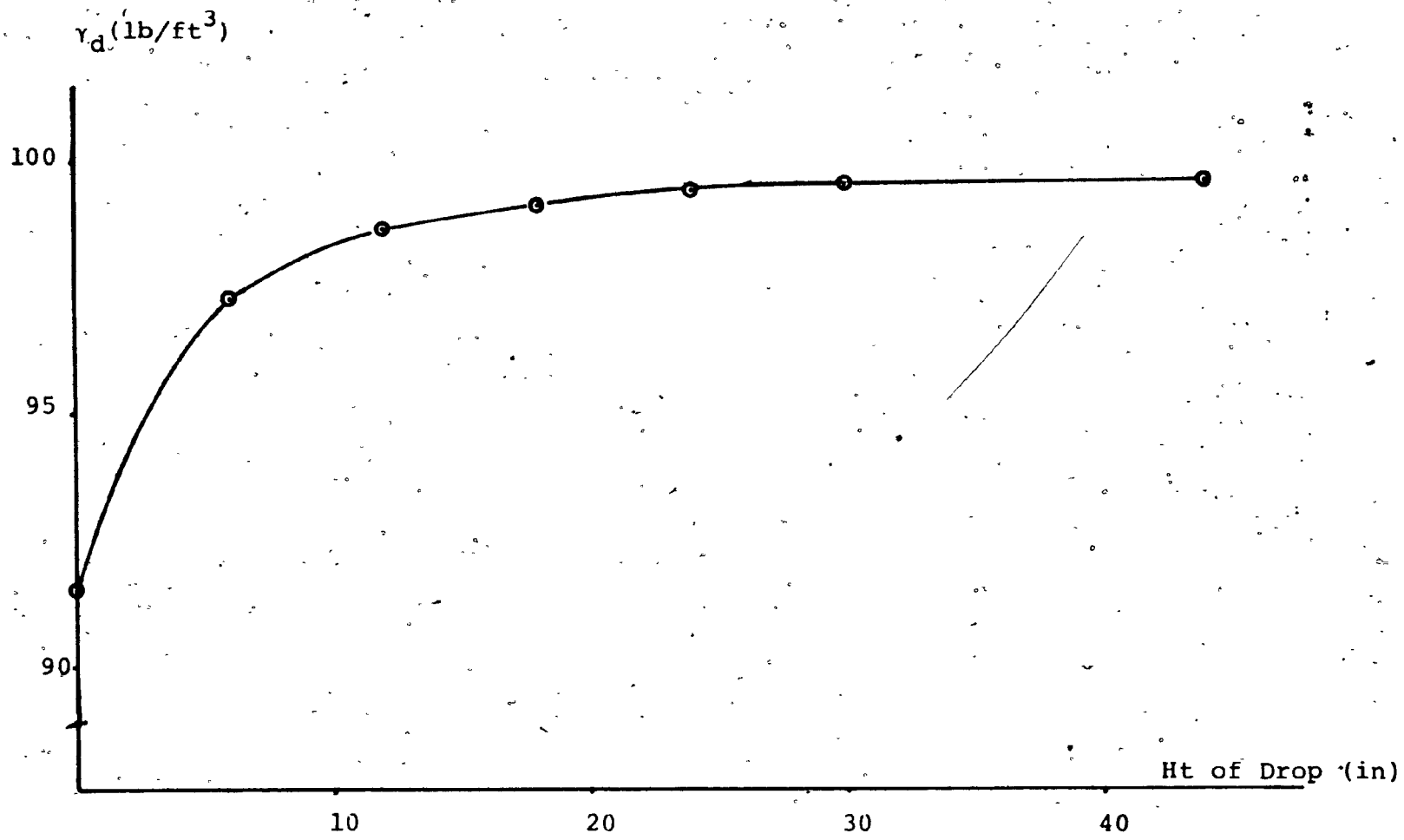


Fig. 3.23: Unit Weight of Sand vs. Ht. of Drop.

# CHAPTER IV

# EXPERIMENTAL RESULTS

## 4.0 General

In the study of foundation engineering problems, full-scale field tests are the ideal method for obtaining data. However practical difficulties and economic considerations either eliminate or considerably restrict the field tests' scope. As an alternative to full scale field tests, carefully conducted model tests may be employed with advantage. Such model tests can provide useful qualitative and some quantitative data which could later be supplemented with some field tests. In addition, there are a number of variables which influence the behaviour of foundations and these can be isolated and studied in detail by means of model tests.

The critical aspect of any research program is to obtain accurate results. Throughout this testing program, utmost care was exercised in all facets of testing to ensure that the quality of the data be of the highest degree possible.

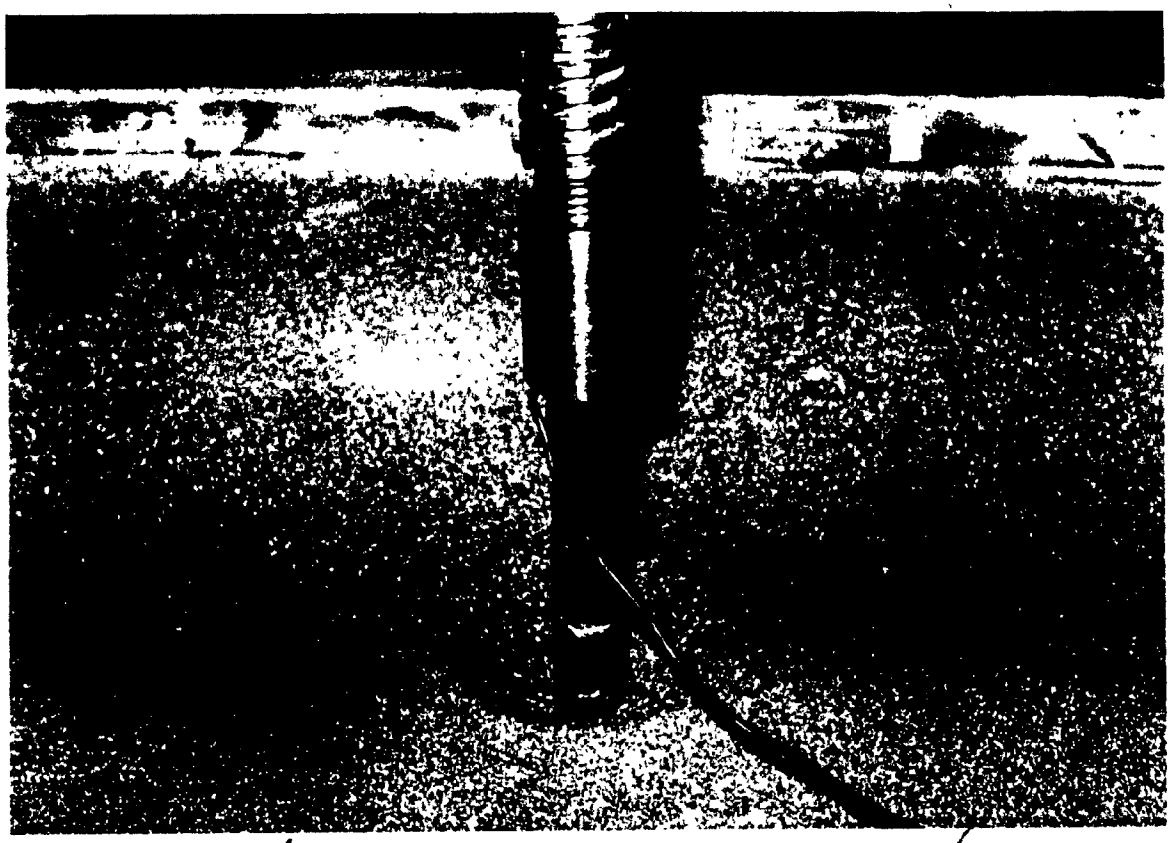

Figure 4.1: Pushing Model Pile 1
into sand

## 4.1 Testing Program And Procedure

Table 4.1 summarizes the testing program for model piles 1 and 2. In each test, the sand is spread into the box from an elevation of at least 44 inches. This results in a uniform bed of sand with a unit weight of $\gamma$=99.59 lb/ft$^3$. To check for this unit weight during the test, two sand pots are placed at two different elevations in the box and they are carefully removed and weighed after each test. The results are verified and show good agreement with the calibration values.

After adjusting the loading column to the desired angle, the model pile is pushed into the sand (Fig. 4.1 & 4.2) at a rate of 1.0 inch per minute to the selected depth. It is then unloaded for mounting a load measuring unit at the pile top. After initial readings are recorded, the pile is pulled at a constant uplift rate of 0.01 inch per minute. At a pile displacement equal to at least 30 percent of pile diameter, the pile is unloaded and then removed.

Model pile 1 is pushed 60 inches into the sand, proving ring readings and pile displacements are recorded at regular intervals during the load test (Fig. 4.3).

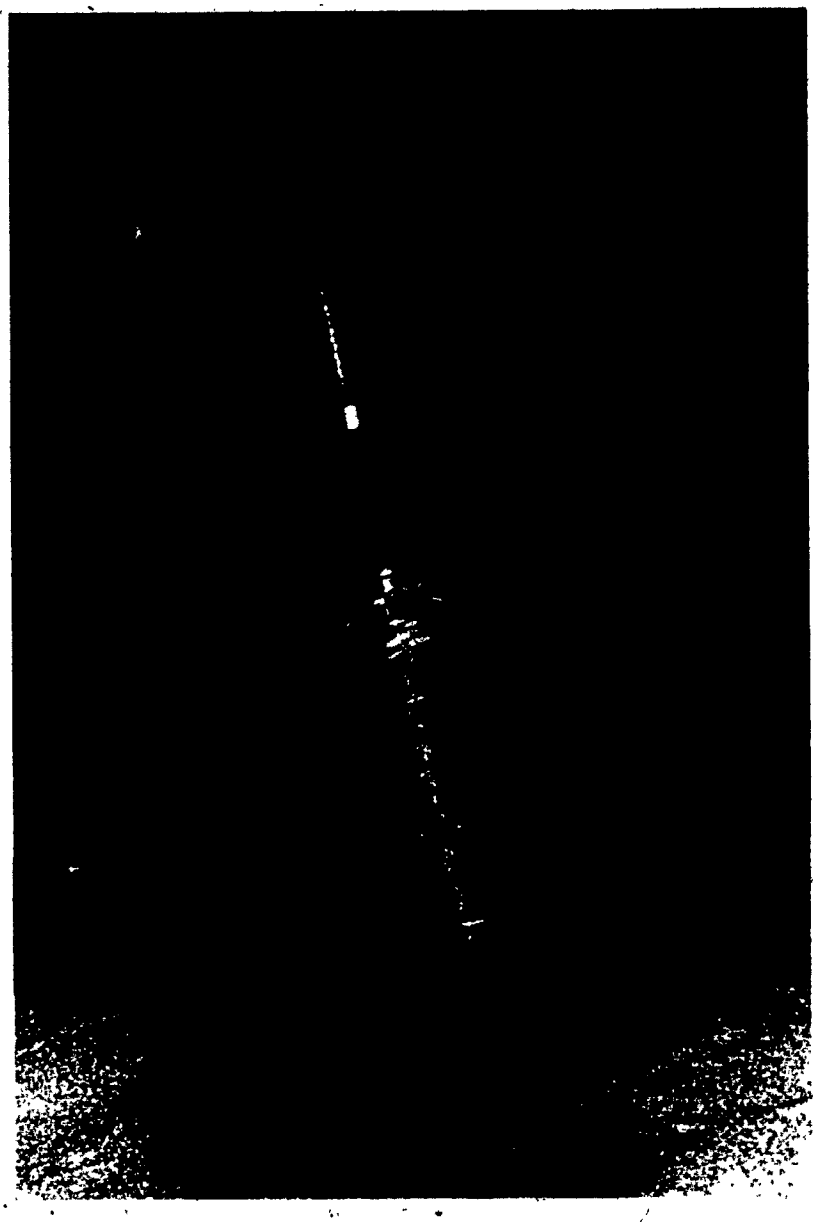

Figure 4.2: Pushing Model Pile 2 into sand.

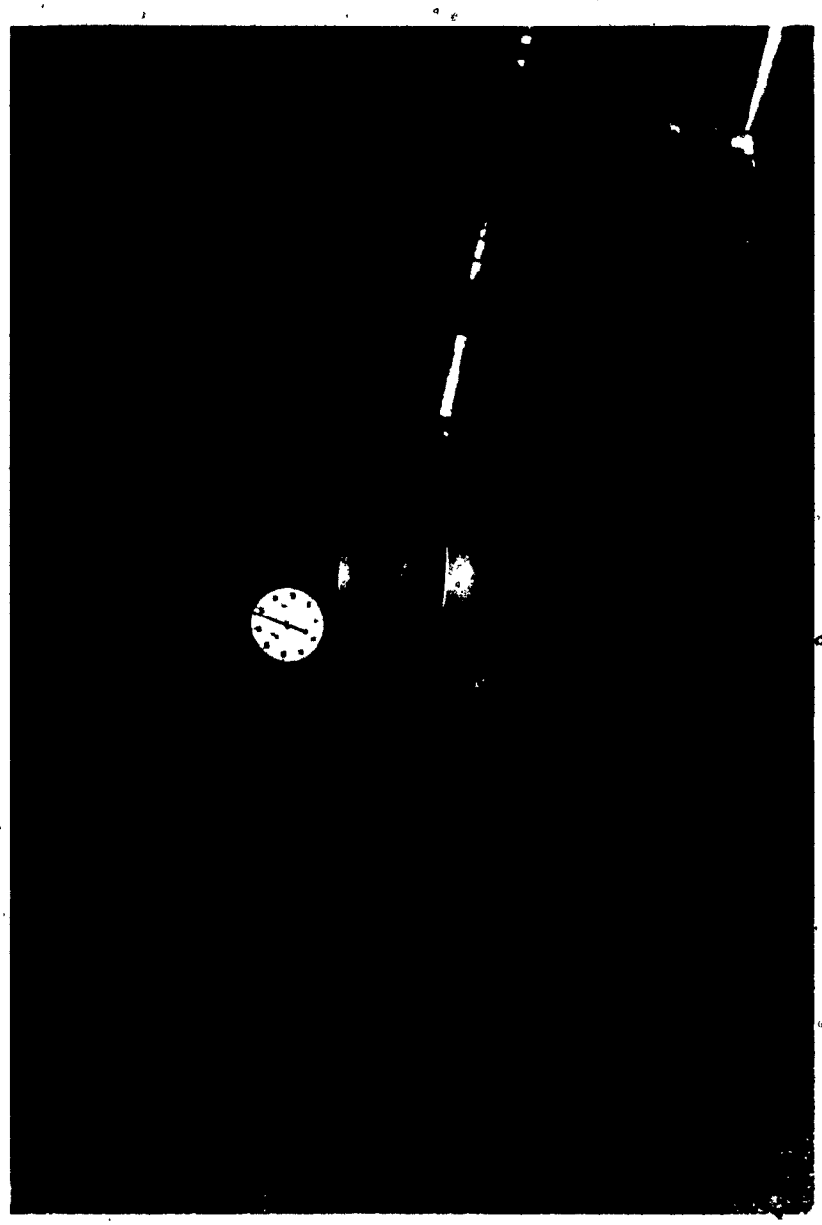

Figure 4.3: Pulling of Model Pile 1.

Model pile 2 is pushed 61.5 inches into the sand, load cell readings at the top of the pile are recorded by means of a data acquisition system (Fig. 4.4) at selected time intervals for the entire test duration (Fig.'s 4.5 & 4.6).

Pile displacements are recorded by the use of dial gages.

SUMMARY OF TEST PROGRAM

| Size of Pile | Test No | Angle of Inclination (in deg.) | Data Sought |
|---|---|---|---|
| 1.5" | 1 | 0 | Displacement of Pile Top. Total load using a proving ring. |
| | 2 | 10 | |
| | 3 | 20 | |
| | 4 | 30 | |
| 3.0" | 5 | 0 | Displacement of Pile Top. Total pullout load using data acquisition system's reading of load cell. |
| | 6 | 15 | |
| | 7 | 30 | |

Table 4.1

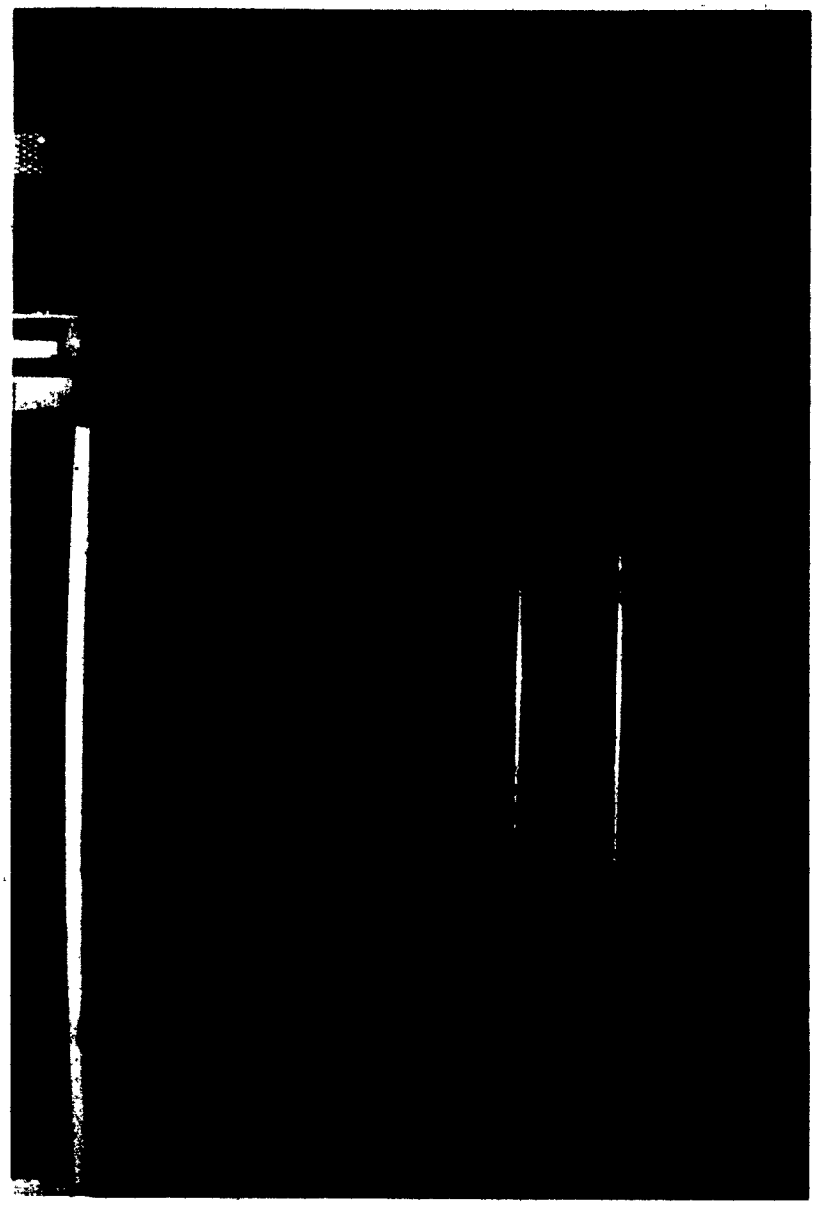

Figure 4.4: Data Acquisition System.

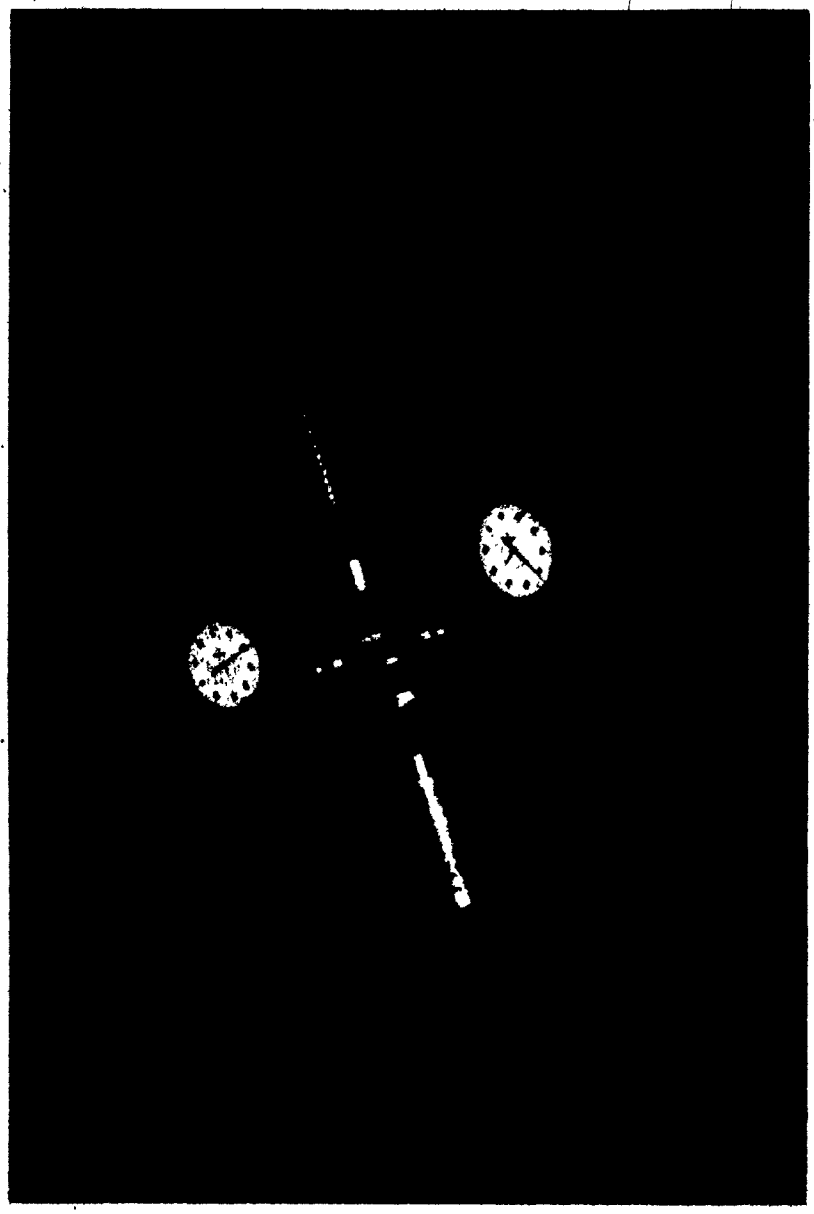

Figure 4.5: Pulling of Model Pile 2.

Figure 4.6: Pulling of Model Pile 2
(with loading system shown).

## 4.2 Calibration of Proving Ring

A proving ring with a capacity of 1000 lbs. in tension is used in this investigation. (Fig. 4.7) shows the calibration of this proving ring.

## 4.3 Results of the Uplift Test On Model Pile 1

Figures 4.8 through 4.11 show the results of the uplift load of the 1.5" pile with an angle of inclination varying between $0^{o}$ and $30^{o}$ respectively.

## 4.4 Calibration Of The Load Cell

The load cell used in this investigation is a flat cell. The Calibration is shown on table 4.2.

Load Cell Calibration

| Load (lbs) | Reading |
|---|---|
| 0 | +1 |
| 500 | 151 |
| 1000 | 301 |

Table 4.2.

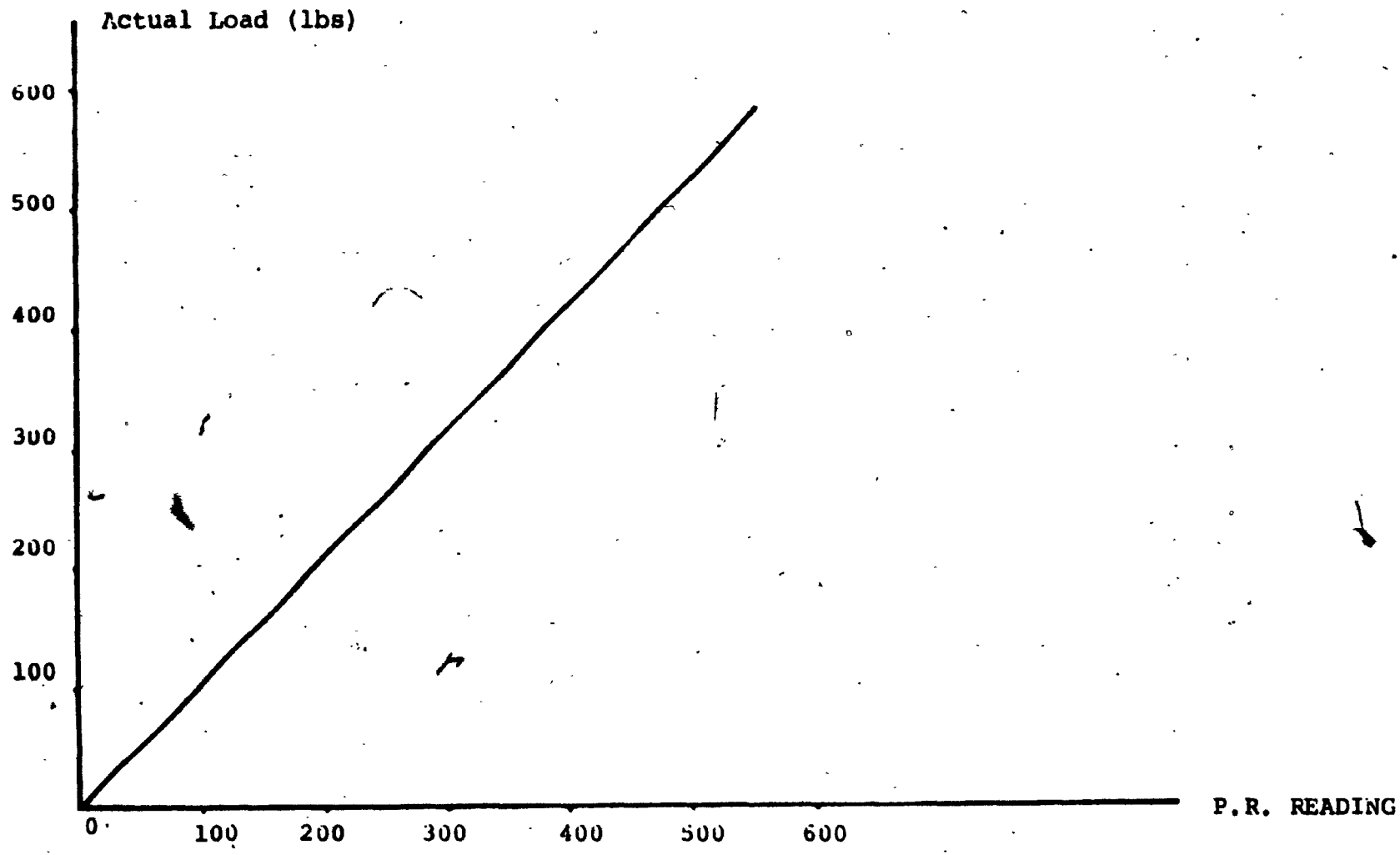


Fig. 4.7: Calibration Curve of Proving Ring

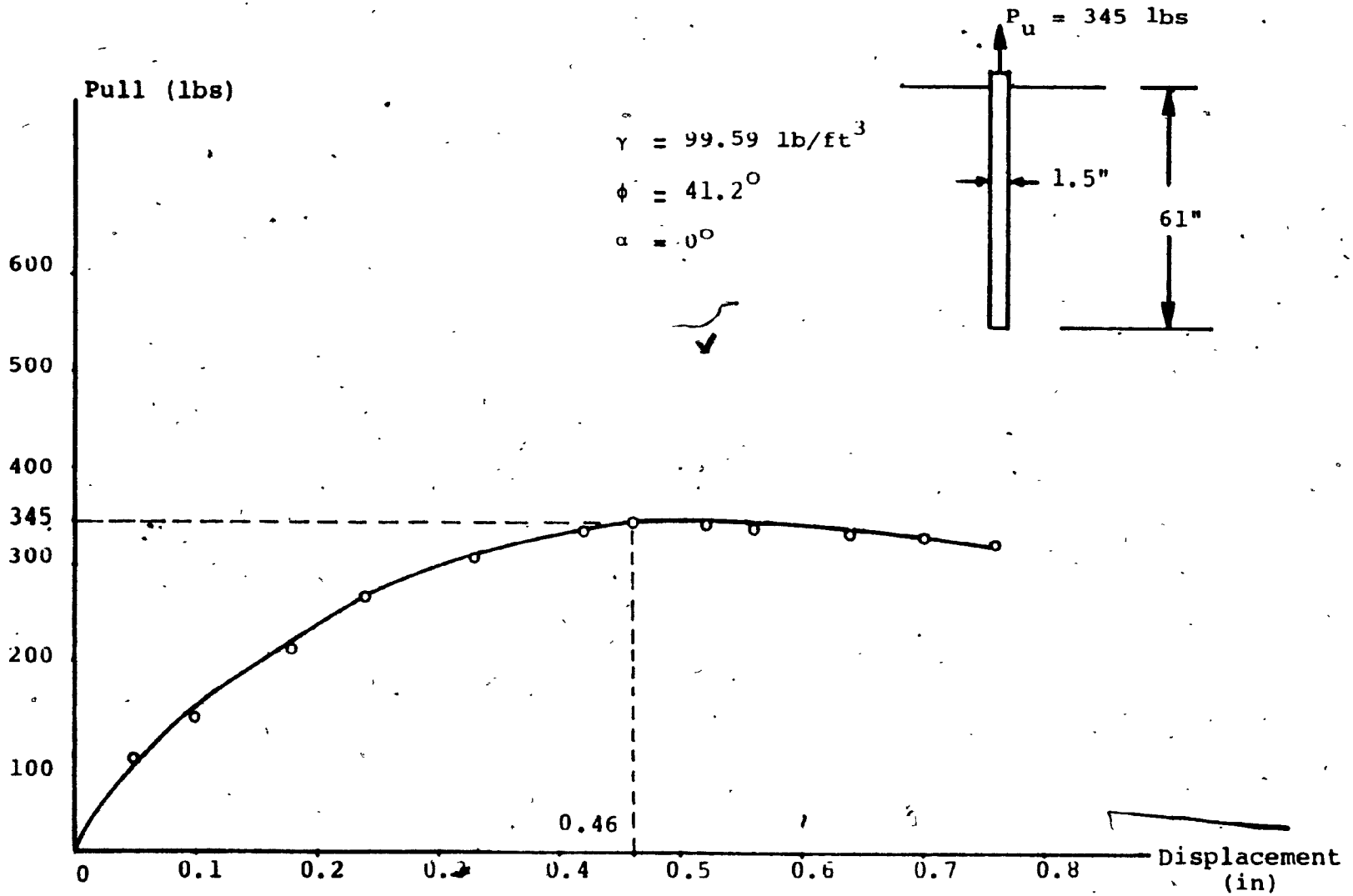


Figure 4.8: Pull-out Capacity vs. displacement of Model Pile 1 with $\alpha = 0°$

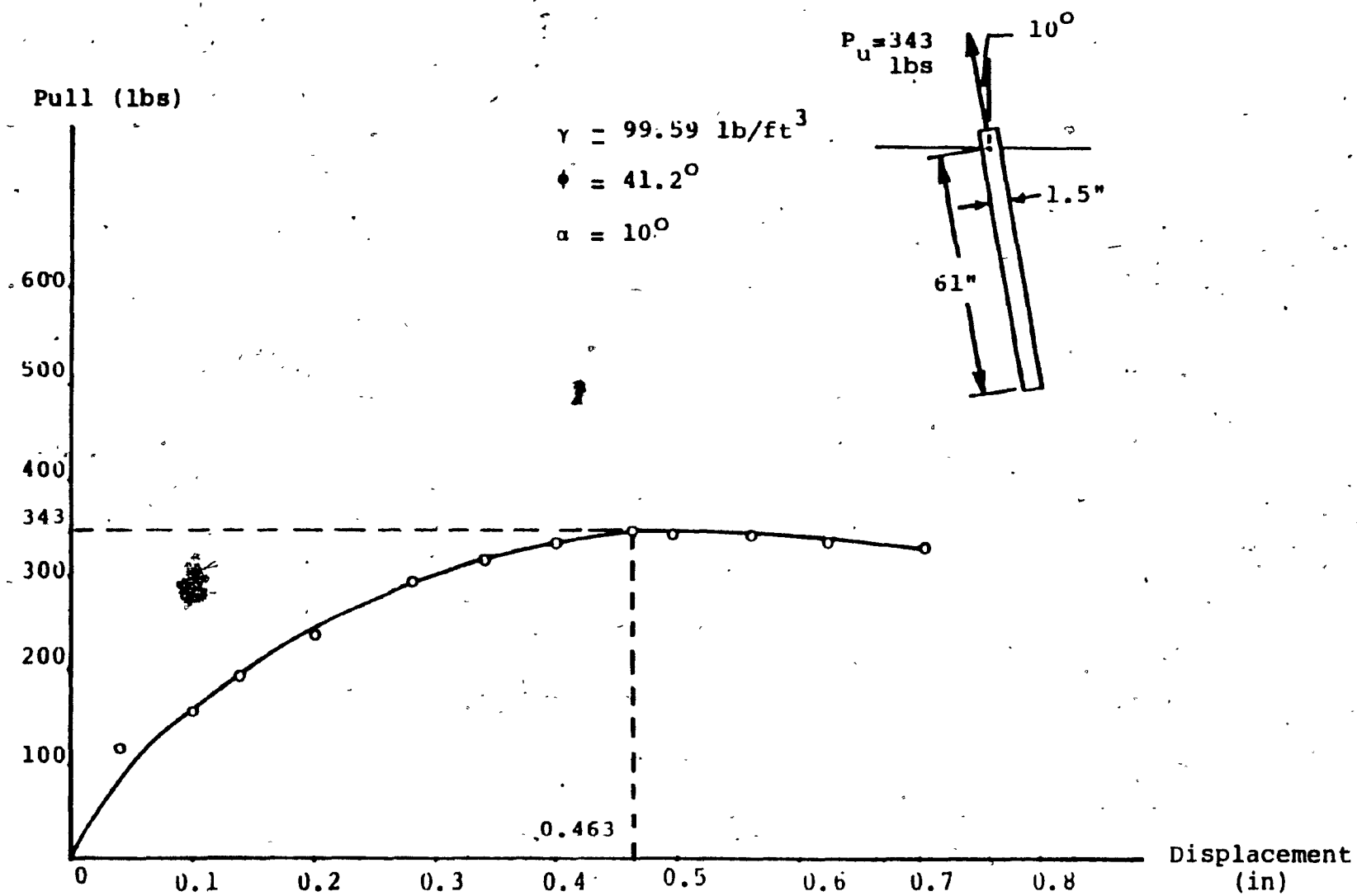


Fig. 4.9: Pull out Capacity vs. displacement of Model Pile 1 with $\alpha = 10^{\circ}$

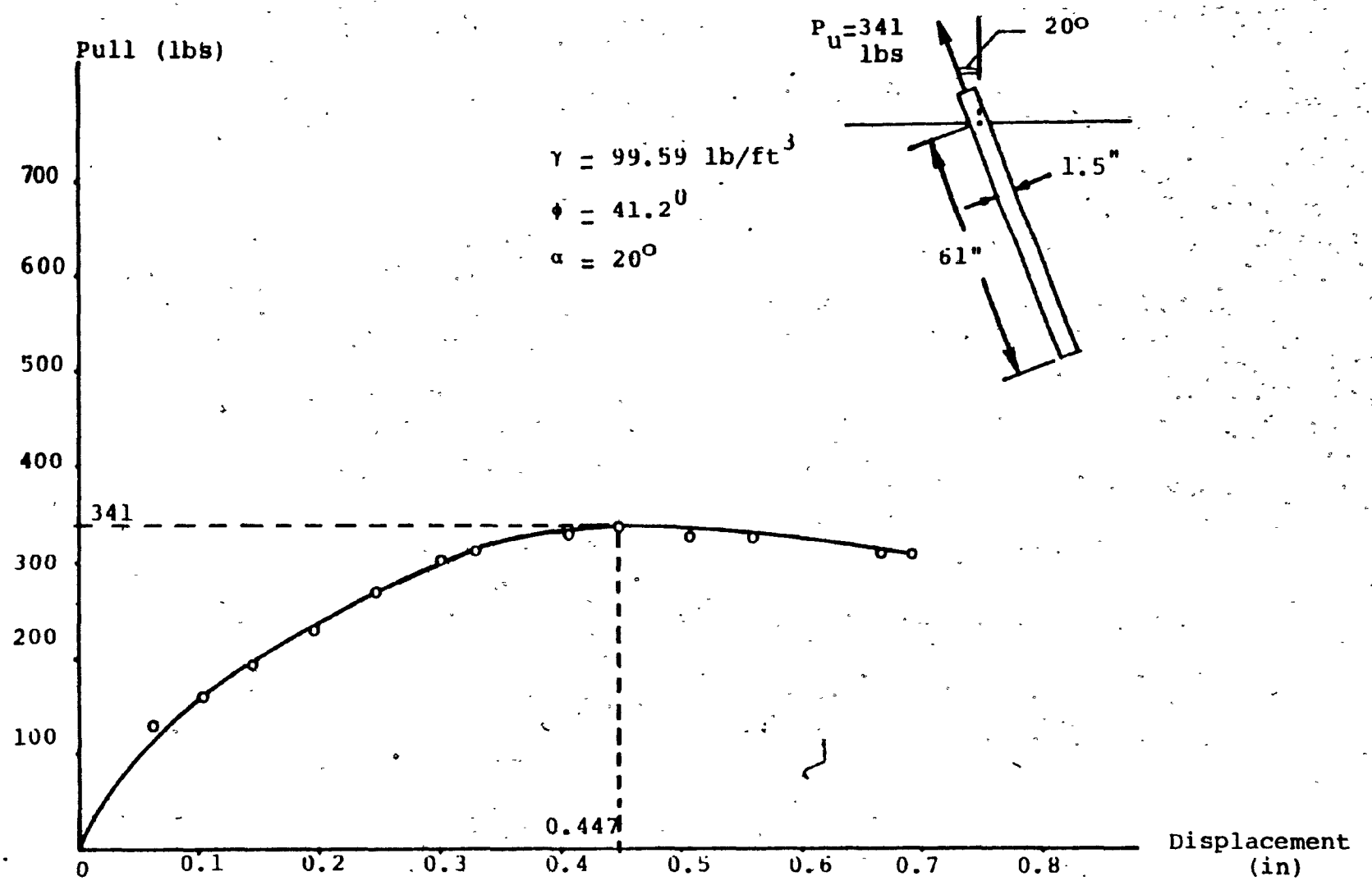


Fig. 4.10: Pull out Capacity vs. displacement of Model Pile 1 with $\alpha = 20^{o}$

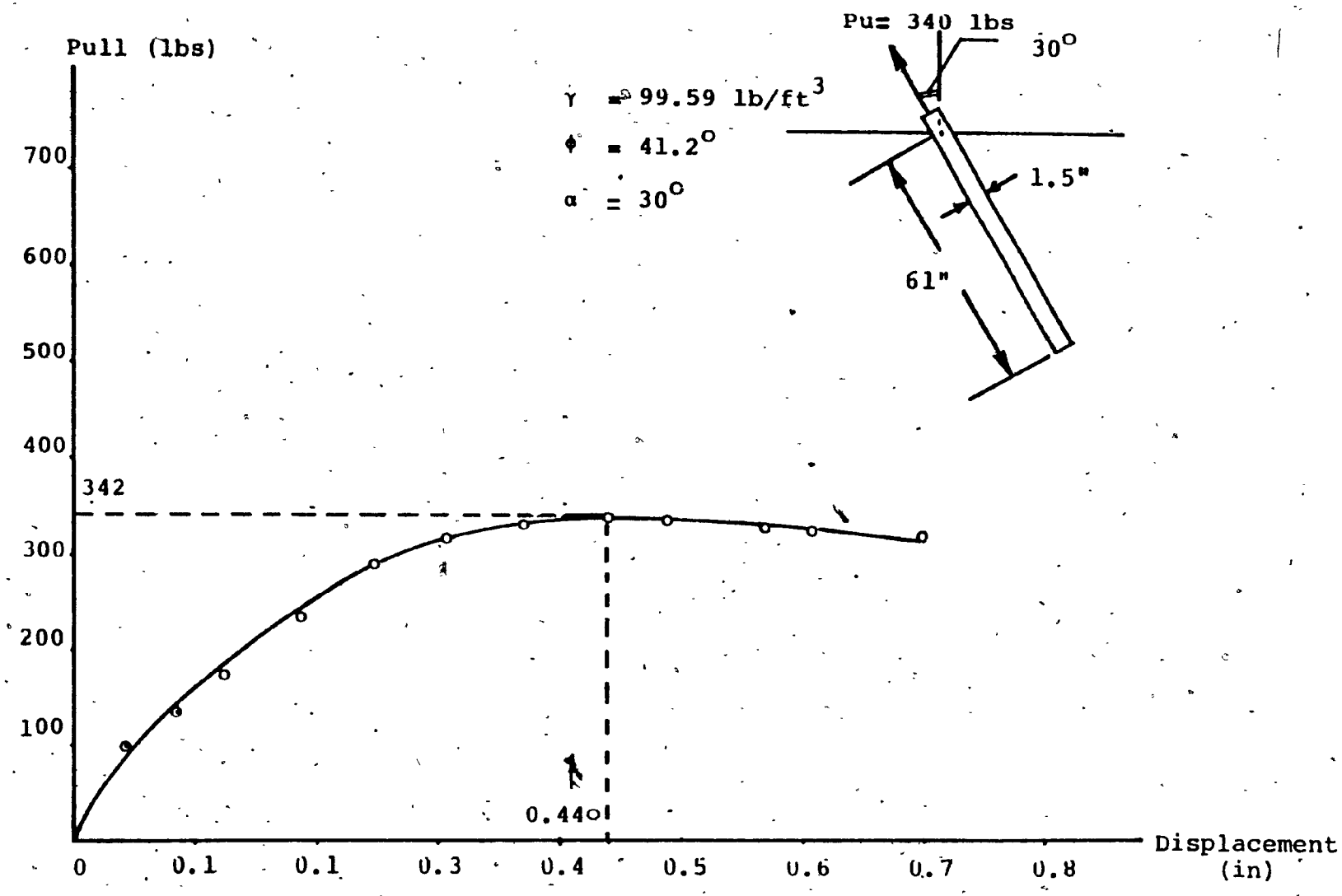


Fig. 4.11: Pull out Capacity vs displacement of model Pile 1 with $\alpha = 30^{\circ}$

## 4.5 Results of the Uplift Test on Model Pile 2

Figures 4.12 through 4.14 show the results of the uplift load of the 3" pile with an angle of Inclination of $0^{o}$, $15^{0}$ and $30^{o}$.

Table 4.3 Summarizes the results of all the tests.

SUMMARY OF TEST RESULTS

| Size of Pile | Angle of Inclination | Max Pull-out Load (lbs.) | Wt. of Pile (lbs.) | Net ultimate Pull-out (lbs.). |
|---|---|---|---|---|
| 1.5" | $0^{o}$ | 345 | 15.53 | 329.47 |
| 1.5" | $10^{o}$ | 343 | 15.53 | 327.47 |
| 1.5" | $20^{o}$ | 341 | 15.53 | 325.47 |
| 1.5" | $30^{o}$ | 340 | 15.53 | 324.47 |
| 3.0" | $0^{o}$ | 795 | 36.45 | 758.55 |
| 3.0" | $15^{o}$ | 787 | 36.45 | 750.55 |
| 3.0" | $30^{o}$ | 771 | 36.45 | 734.55 |

TABLE 4.3

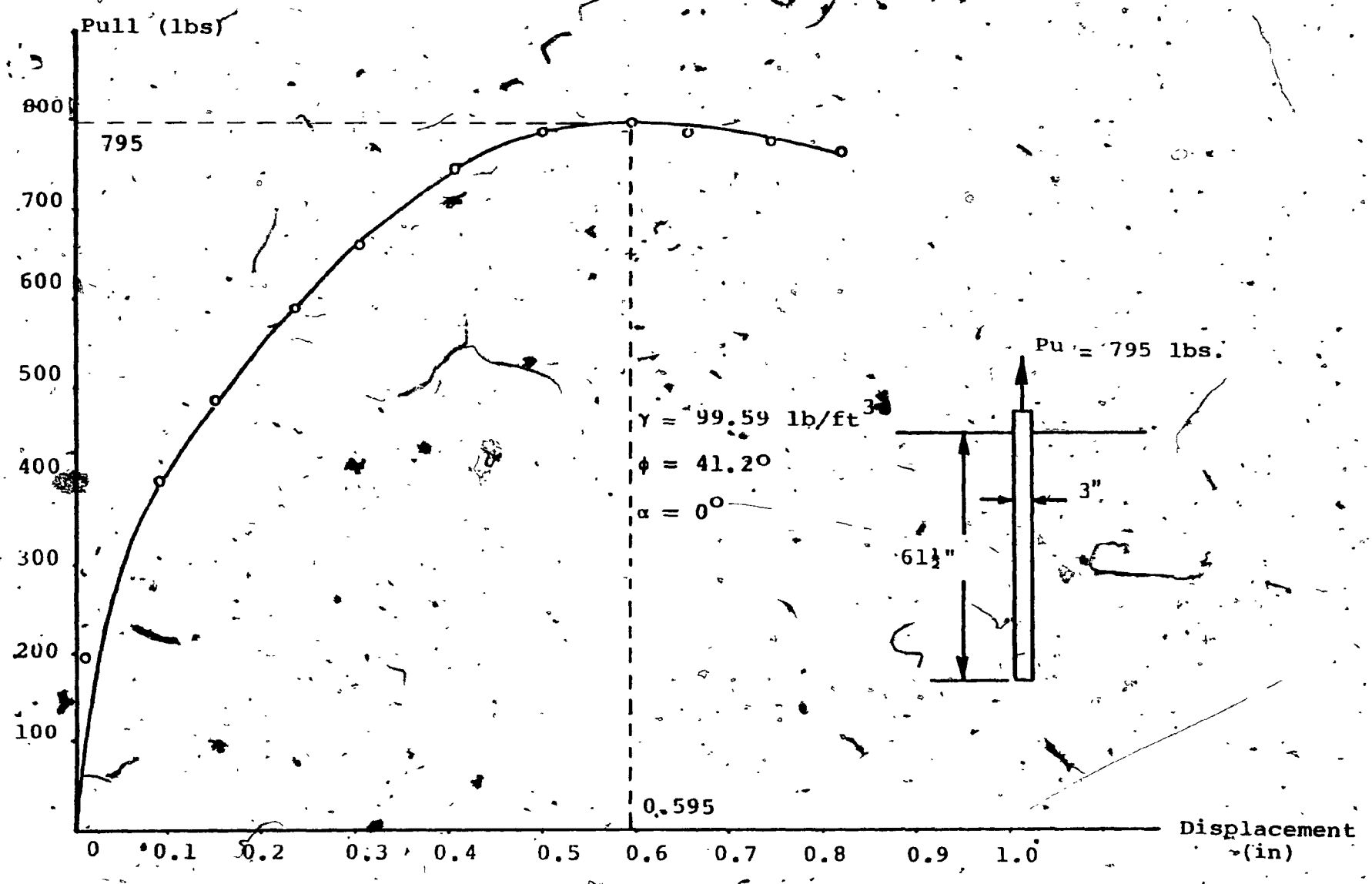


Fig. 4.12: Pull-out Capacity vs. displacement of Model Pile 2 with $\alpha = 0^{\circ}$

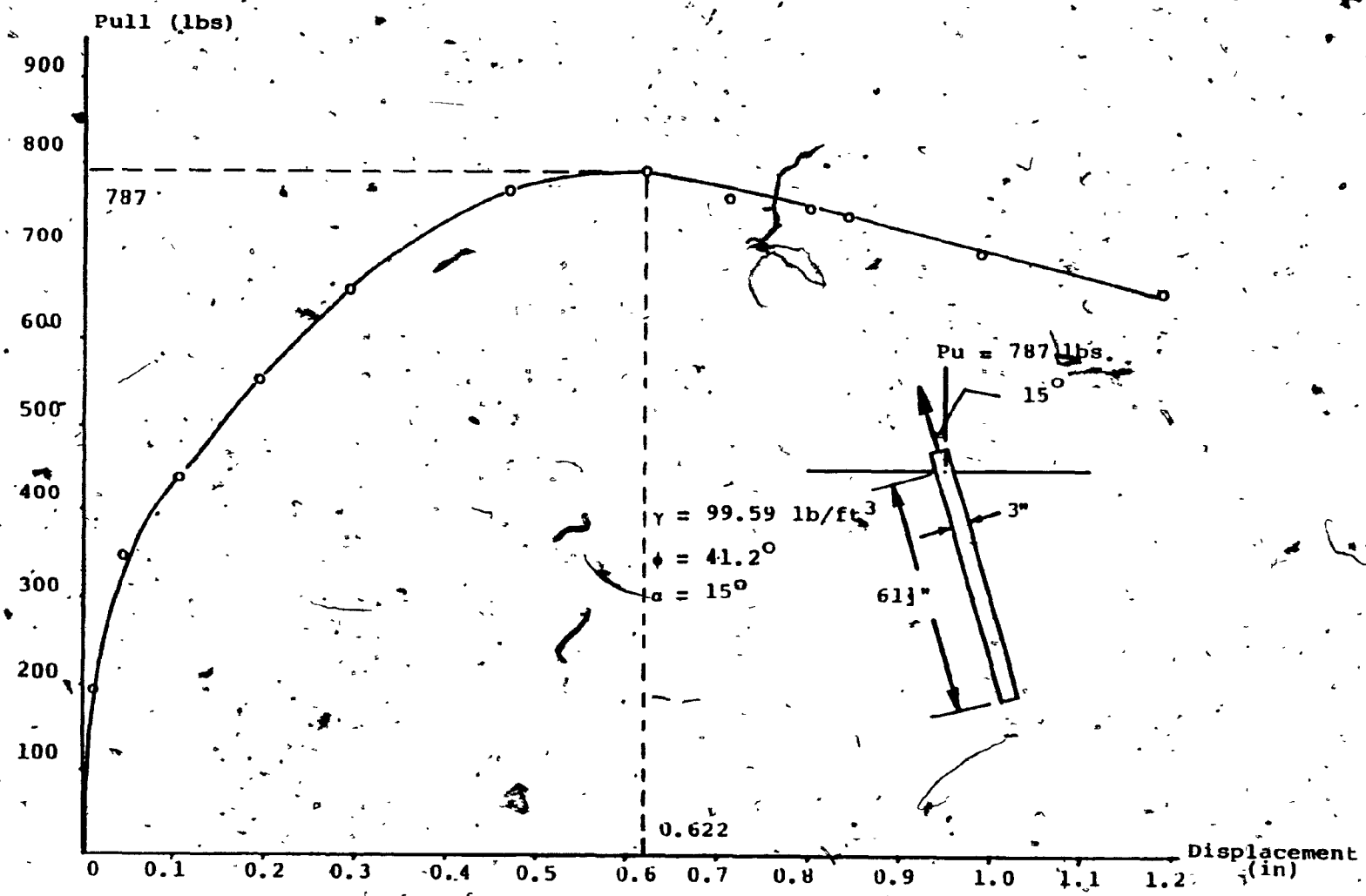


Fig. 4.13: Pull-out Capacity vs. displacement of Model pile 2 with α = 15°

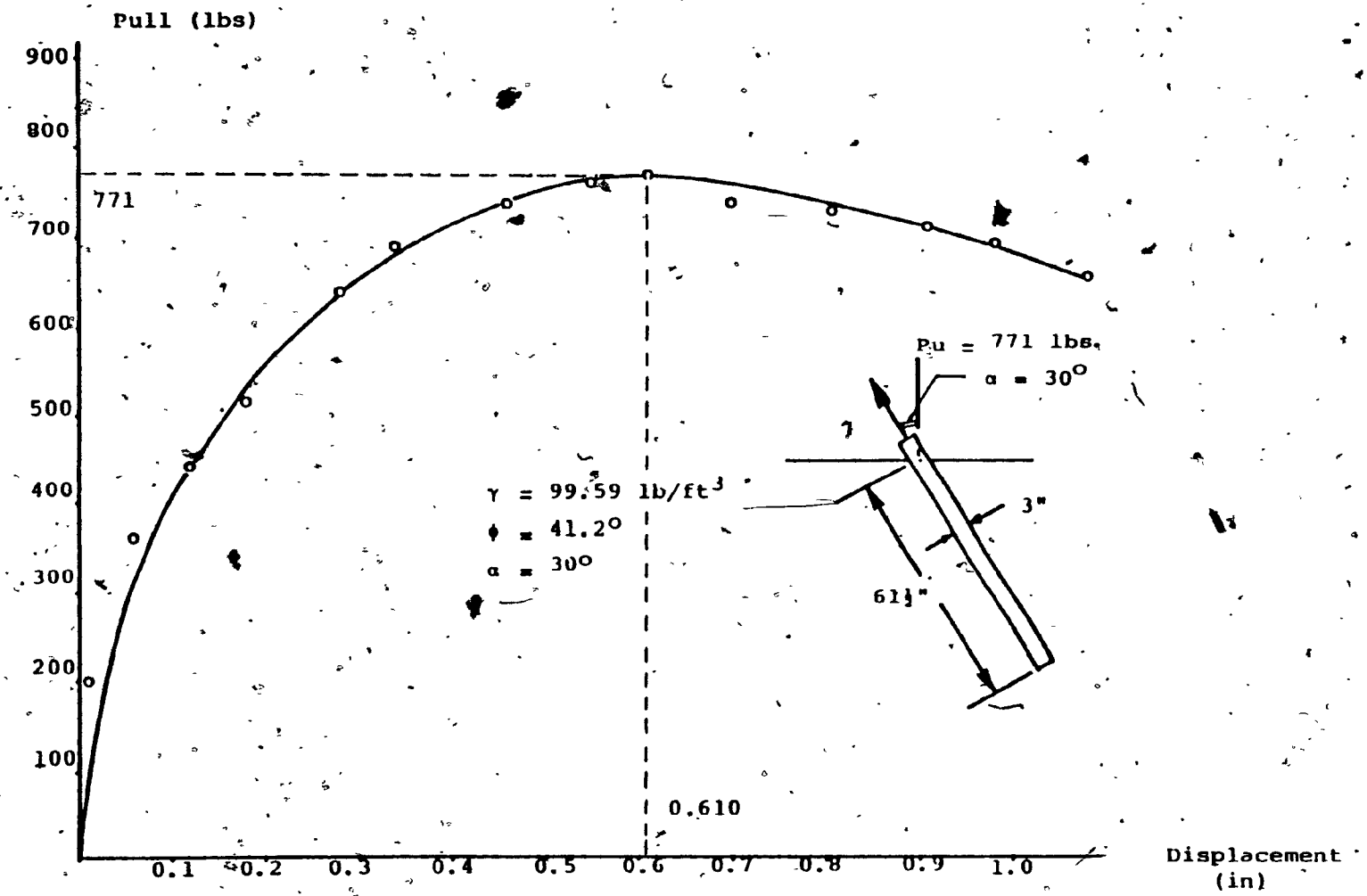


Fig. 4.14: Pull-out Capacity vs. displacement of Model Pile 2 with α 30°

# CHAPTER V

## ANALYSIS OF THE TEST RESULTS

### 5.0 General

The gross ultimate uplift capacity of a single pile driven in a homogeneous sand deposit can be expressed in terms of uplift skin friction plus the weight of the pile.

Thus, $P_u = P_o + W_p$ 5.1

where $P_o$ = Net ultimate uplift capacity of pile

$W_p$ = Self weight of pile.

Because of the complex form of the failure surface, no exact method is available to compute the shear distribution and uplift capacity of a drilled shaft. The most common and widely accepted method, especially among the practicing engineers, is the cylindrical shear model (13,22). Equation (5.1) can be expressed as follows:

$$P_u = \pi D \frac{L^2}{2} K_u \gamma' \tan \phi' + W_p \qquad 2.7$$

The key element in the successful use of this approach is the determination of K at failure. In granular soils four theoretical values of K are possible. These values are based on the various possible stress deformation responses of the soil during shaft construction. On this basis, one value of K could be $K_o$, the coefficient of earth pressure at rest. The second possible value of K is $K_a$, the coefficient of Rankine earth pressure. For a loose soil with void ratio greater than the critical value, relaxation of the soil would be expected, and the K value may approach the $K_a$ value. The $K_a$ value is based on the assumption that the yielding of the soil toward the shaft casing is two-dimensional. But the actual soil yielding may be three-dimensional and as yielding occurs, arching in a horizontal plane may develop. Therefore, the third and lowest possible value of K may be that corresponding to the fully developed arching case. The fourth and highest value of K could be greater than $K_o$. This value may be obtained if the void ratio of the soil is less than the critical value.

Considering that the surface may be rough, shearing

at this surface will cause dilation of the soil and thus a portion of the passive resistance will be mobilized. Therefore, for a dense, granular soil, a relatively high value of K may be expected.

The selection of an appropriate K value is not straightforward because of a complex failure mechanism. Using simplified assumptions, Meyerhof (15,16) presented a general theory for calculating the uplift capacity of piles.

## 5.1 General Uplift Theory

A state of general shear failure exists along the failure surface on which a friction force F is mobilized (Fig. 5.1) based on a unit shearing resistance

$$t_f = \sigma \tan \phi \qquad 5.2$$

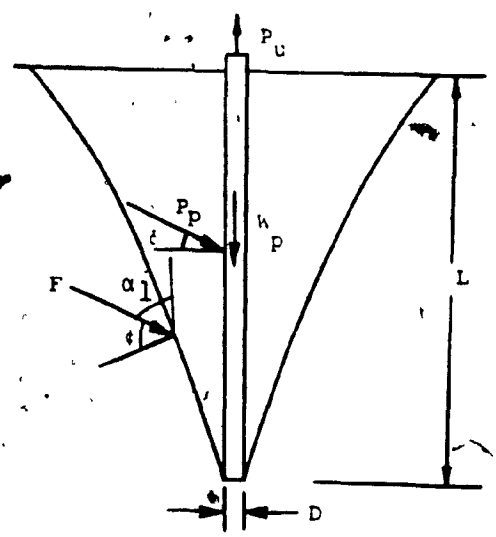


Fig. 5.1 Failure of soil under uplift load.

where $\sigma$ = Normal stress on failure surface

$\phi$ = Angle of internal friction of soil

Hence the ultimate uplift load of pile per unit length $P_u = 2F \overline{\cos \alpha_1} + W_p$ 5.3

where $\alpha_1$ is the average inclination of force F with the vertical.

In the absence of a rigorous solution for the stresses on the failure surface it may be assumed that $P_u$ is approximately given by

$$P_u = P_p \sin \delta \, \pi D + W_p \qquad 5.4$$

where $P_p$ = Total passive earth pressure inclined at average angle $\delta$.

Expressing the normal component of $P_p$

$$P_p \cos \delta = \gamma (L^2/2) K_u \qquad 5.5$$

where $\gamma$ = unit weight of soil,

and $K_u$ = uplift coefficient

Equation 5.4 becomes

$$P_u = \gamma L^2/2 \tan \delta \, K_u \pi D + W_p \qquad 5.6$$

## 5.2 Analysis of Uplift Capacity of Vertical Piles

a) 1.5" diameter vertical pile

Using equation (5.6)

and substituting the values of D = 1.5", L = 61"

$\gamma$ = 99.59 lb/ft$^3$, $W_p$ = 15.3 lbs. and $P_u$ = 345 lbs.

$$345 = 1/2\ \pi\ (1.5)(61)^2 \times \frac{99.59}{(12)^3} \times K_u \times \tan\delta + 15.53$$

Hence 329.47 = 505.3 $K_u \tan\delta$

or $K_u \tan\delta$ = 0.65

where Net uplift capacity = $P_o$ = 329.47 lbs.

If the analysis is made on the actual curved planes of failure, the angle $\delta$ will be equal to $\Phi$. If however, the analysis is made on the assumed vertical planes, the angle $\delta$, mobilized must be less than $\Phi$ as failure has not taken place on the actual planes (17).

From the corresponding passive earth pressure coefficients, $K_p$, based on curved failure surfaces (6), and by trial and error, the values of $\delta$ and $K_u$ are established approximately as 16 and 2.33 respectively.

b) 3.0" diameter pile

Using the same equation (5.6) and substituting the values of D = 3.0", L = 61.5", $\gamma$ = 99.59 lb/ft.$^3$

$W_p \equiv 36.45$ lbs. and $P_u = 795$ lbs.

$$795 = 1/2\ \pi(3)(61.5)^2 \times \frac{99.59}{(12)^3} \times K_u \times \tan\delta + 36.45$$

Hence $758.55 = 1027.2\ K_u \tan\delta$ or $Ku \tan\delta = 0.74$

where Net uplift capacity = $P_o$ = 758.55 lbs.

Using the same method of analysis (as for the 1.5" diam. pile) and by trial and error, the values of $\delta$ and $K_u$ are established for this present investigation as 17 and 2.48 respectively.

The value of $\phi$ used in the present analysis is the one from the triaxial test since it best represents the stresses at the assumed curved failure surface.

Hence for a Relative Density of 65.46% the value of $\phi = 39^o$ is obtained from FIG. 3.21.

The values of $\delta$ as established by Meyerhof for the

corresponding $\phi$ values are shown on FIG. 5.2. The present test results show a very good agreement with the established theoretical curve.

For the purpose of comparison, the variation of $K_p$, $\sqrt{K_p}$, $K_o$ and $K_a$ with $\phi$ is plotted along with the uplift coefficients derived by Meyerhof (15) and some available test results FIG. 5.3.

It appears that the present test results fit nicely with Meyerhof's uplift coefficient values.

## 5.3 Analysis of Uplift Capacity for Inclined Piles

The test results (Table 4.3) indicate that the ultimate uplift capacity of inclined piles decreases very little by increasing the angle of inclination, $\alpha$, from $0^o$ to $30^o$.

The net ultimate uplift capacity of inclined piles can be computed by the proposed empirical equation:

$$P_\alpha = P_o \cos(\alpha/2) \qquad 5.7$$

where $0^o \leq \alpha \leq 30^o$

& $P_o$ = Net ultimate uplift capacity of vertical piles

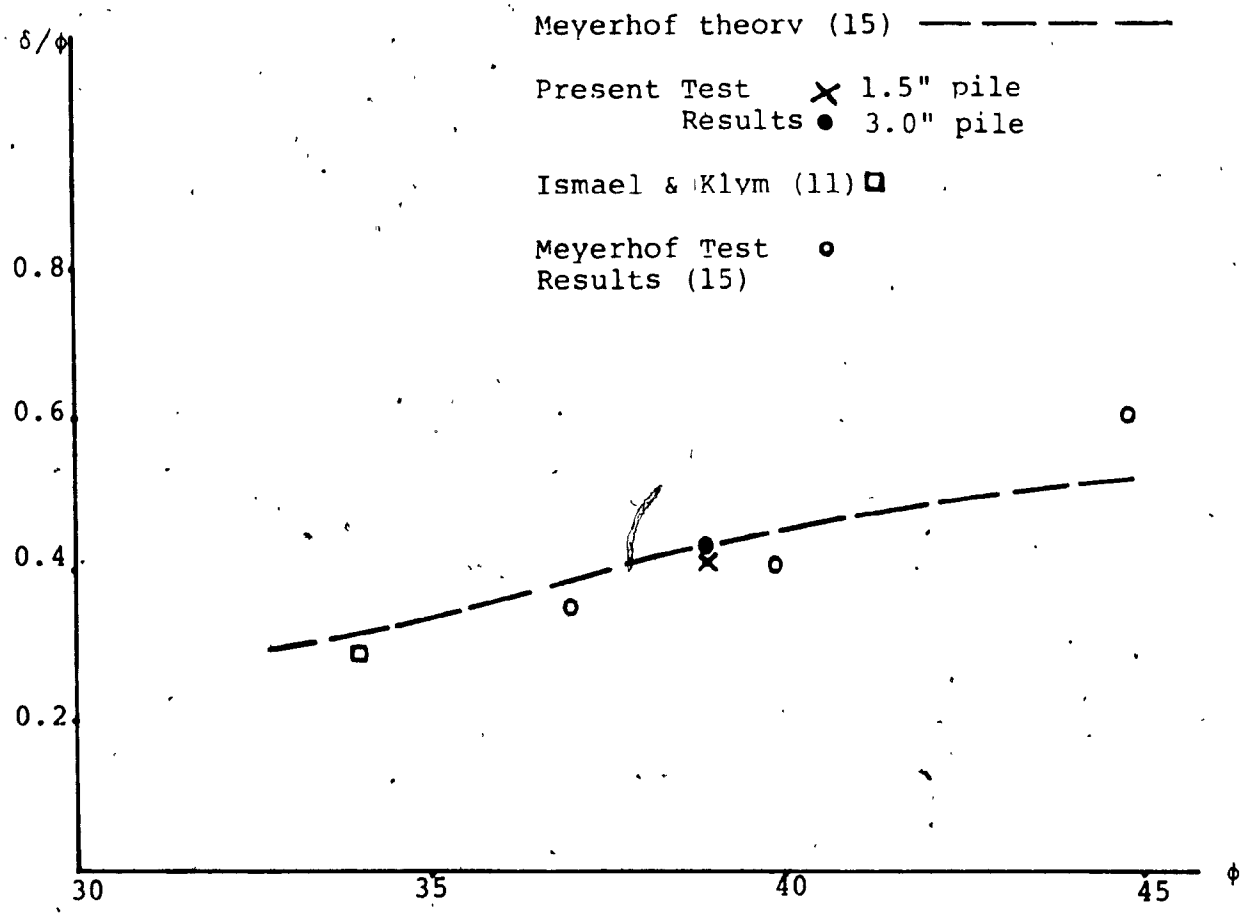


Fig. 5.2 Establishing δ values for given φ.

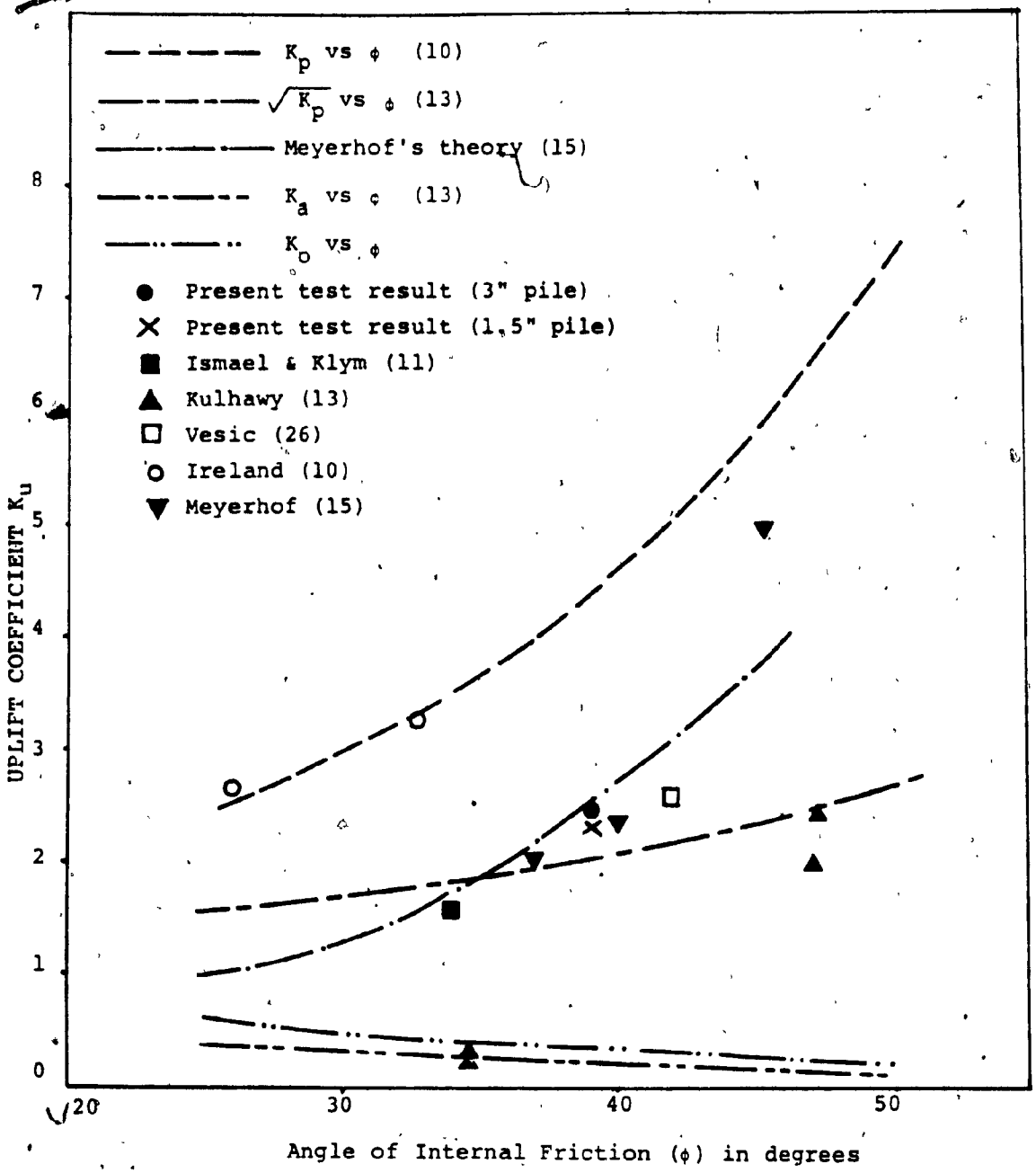


Fig. 5.3: Comparison of theoretical and experimental test results for uplift tests in granular soils.

calculated by using Meyerhof's uplift coefficient.

By applying this equation a good agreement is obtained as shown in (FIG. 5.4).

For the theoretical explanation of this decrease in the uplift capacity, values for the passive earth pressure coefficients, $K_p$, based on curved failure surfaces (11) are established in FIG. 5.5.

To find average values for the uplift coefficient $K_u$, for inclined piles, it is assumed that there is one positive and one negative face for the inclined pile as shown in (FIG. 5.6), the other two faces being unaffected by the inclination i.e. neutral.

FIG. 5.7 shows an example to explain the abovementioned for the 1.5" diameter pile.

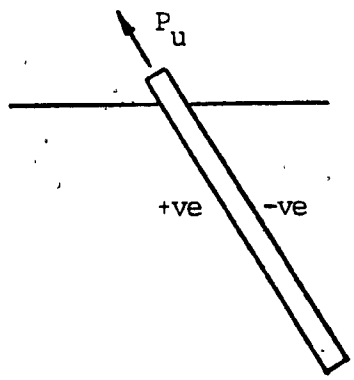


FIG. 5.6 Different faces for inclined piles.

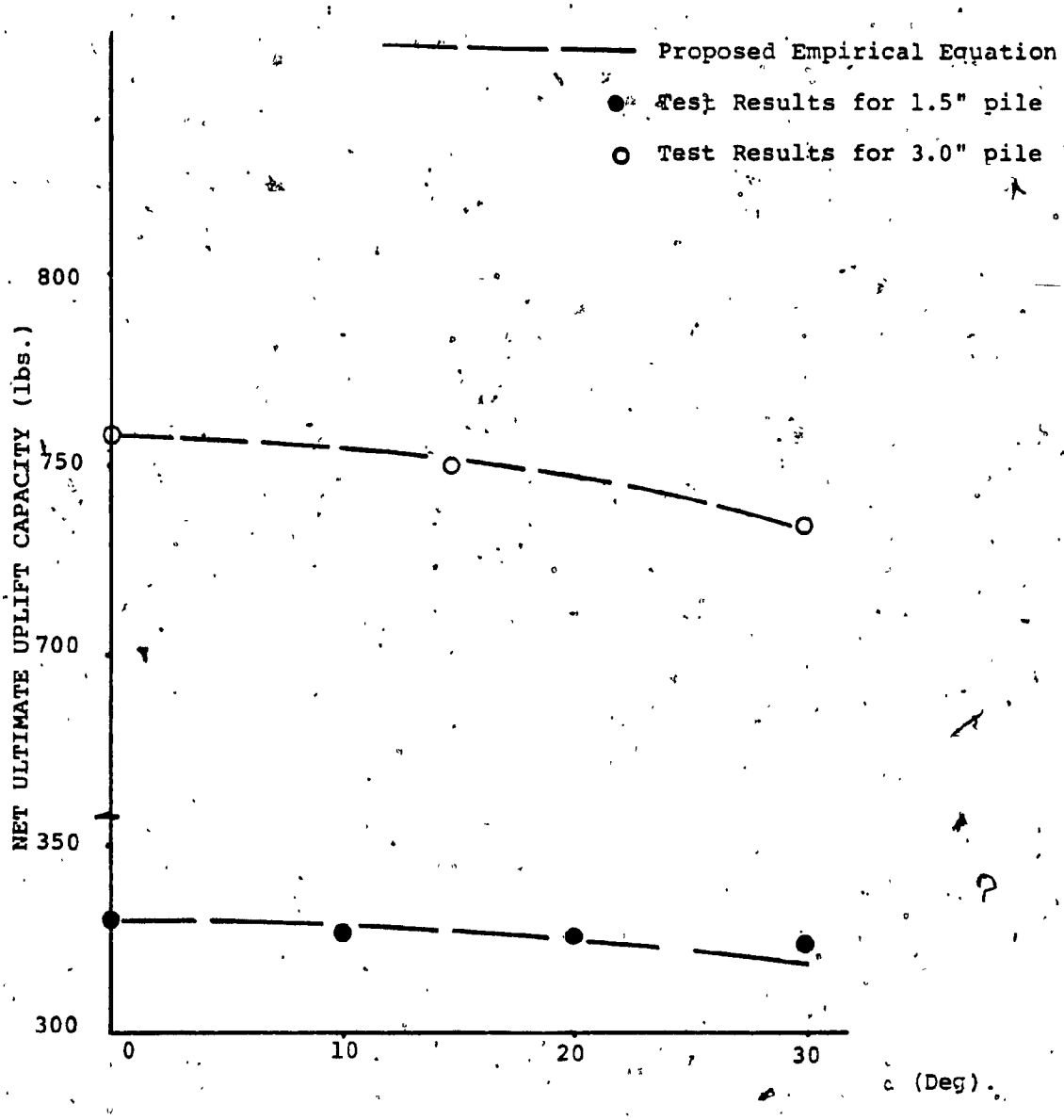


FIG. 5.4: Ultimate uplift capacity of pile vs pile inclinations.

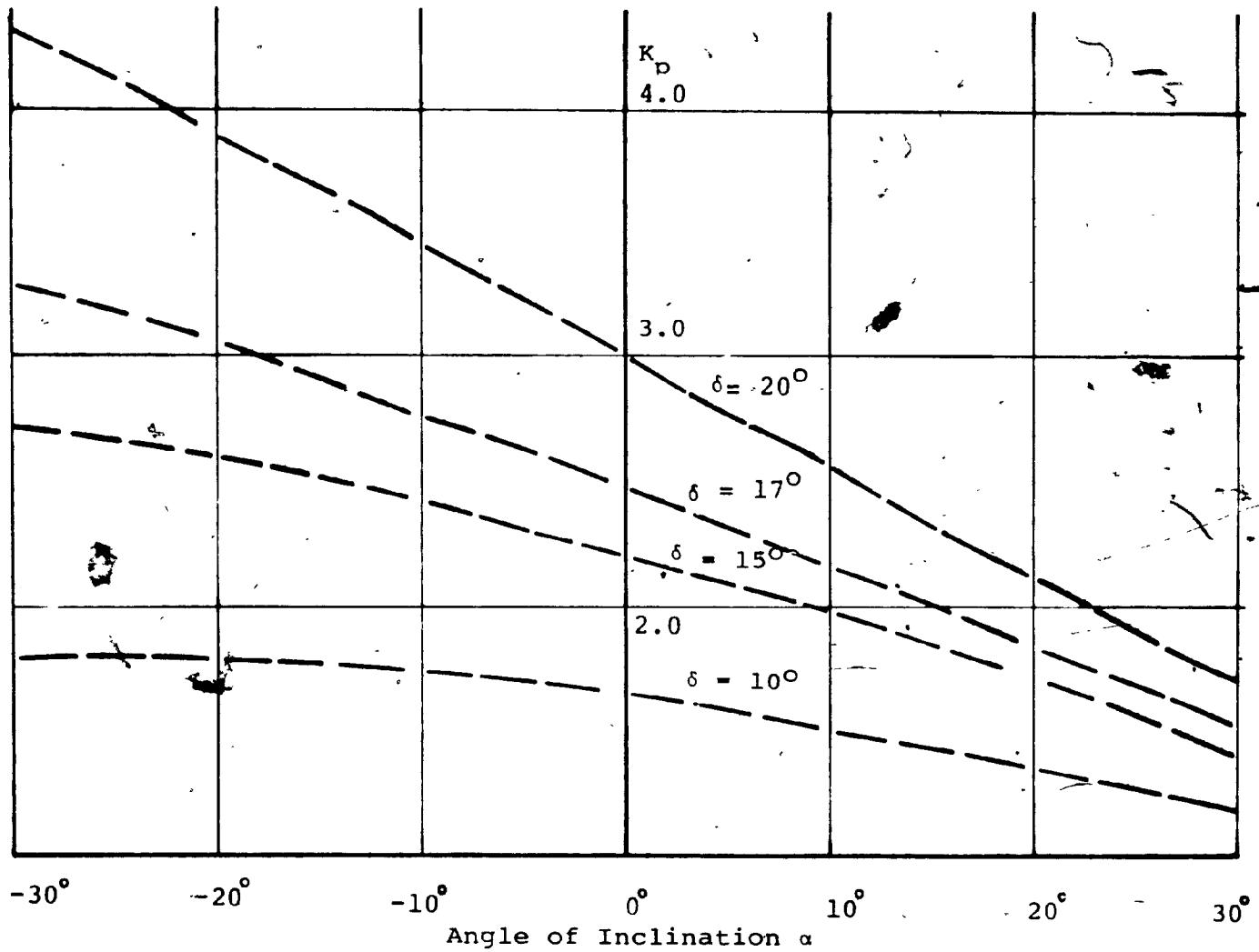


FIG. 5.5 Passive Earth Pressure Coefficient values vs Angle of inclination.

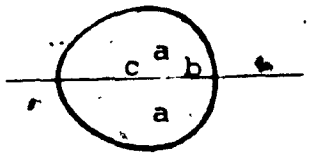


a = neutral face = 2.33

b = positive face = 1.75

c = negative face = 2.80

FIG. 5.7 Passive Earth pressure Coefficient distribution for $\delta = 16^{\circ}$ and with an angle of inclination $\alpha = 20^{\circ}$

Using a parabolic distribution for the coefficient values under different inclinations and by integrating, average values for the uplift coefficient, $K_{u\ (ave.)}$, are established (FIG. 5.8) with the use of Meyerhof's theoretical values (FIG. 5.2).

It appears that the proposed empirical equation (5.7) gives values that fit nicely with the theoretical values derived by using Caquot and Kerisel tables (6) for the passive earth pressure coefficients with values of $\phi$ ranging from $30^{\circ}$ to $40^{\circ}$ and an angle of inclination $\alpha \leq 30^{\circ}$.

The values of the average uplift coefficient are plotted vs. the angle of internal friction in Fig. 5.9.

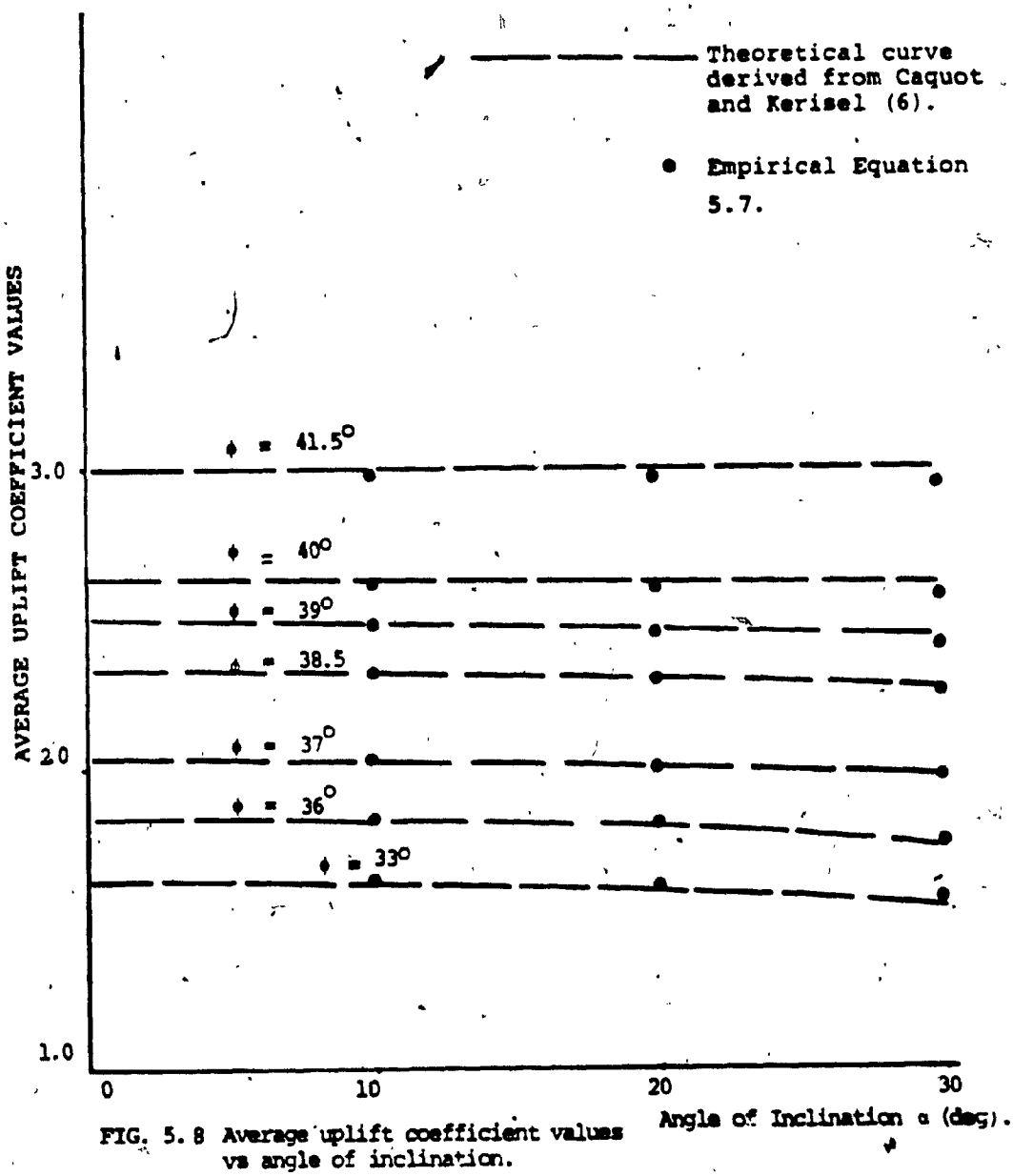


FIG. 5.8 Average uplift coefficient values vs angle of inclination.

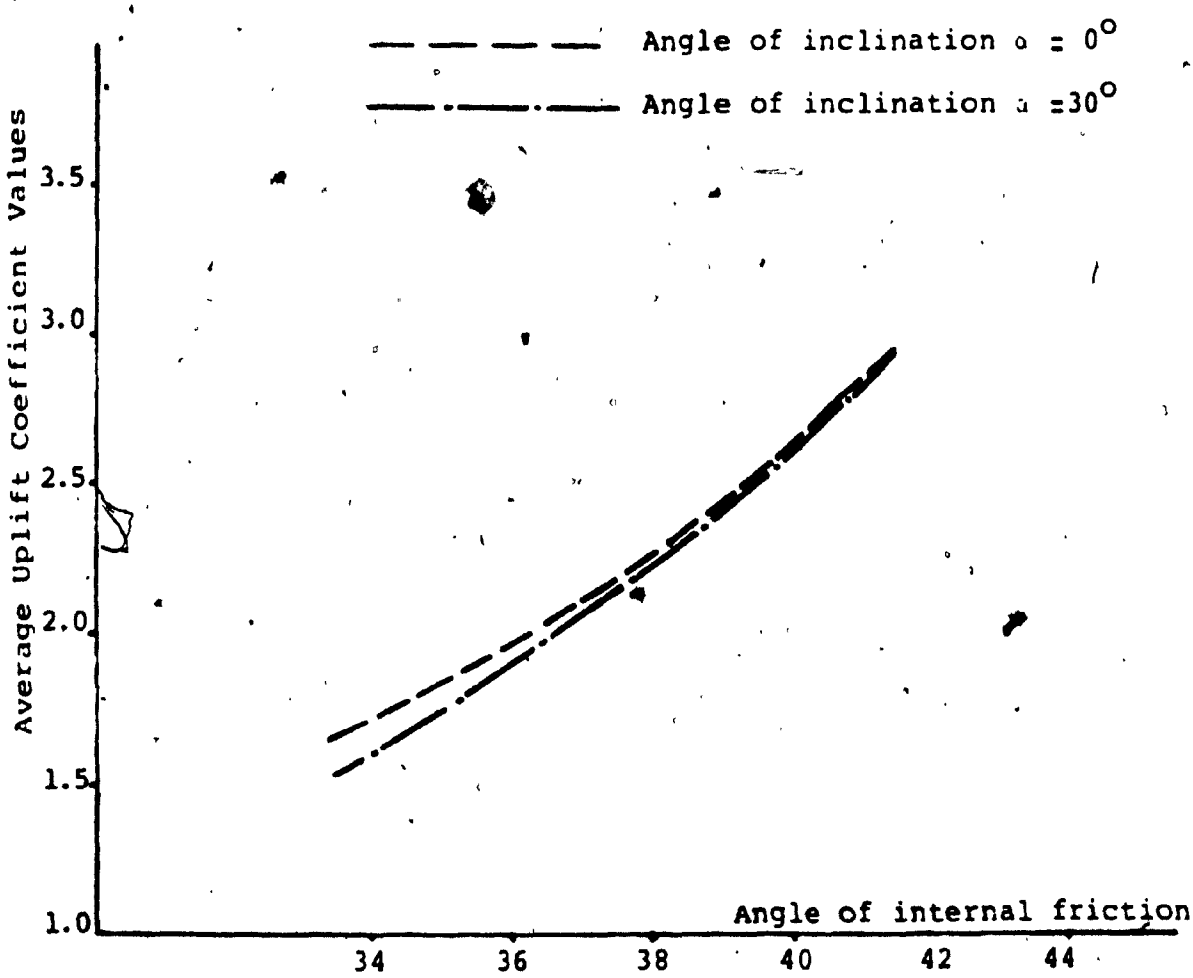


Fig. 5.9 Average Uplift Coefficient Values vs. Angle of Internal Friction

## 5.4 Effect of Pile Size

Table 5.1 shows that the value of the unit skin friction does not change significantly with the increase of the pile diameter from 1.5" to 3.0". This indicates that the scale effects are minimal for the present investigation.

Table 5.1

Variation of unit skin friction with size of the pile.

| | UNIT SKIN FRICTION | |
|---|---|---|
| | Angle of Inclination $\alpha = 0^{\circ}$ | Angle of Inclination $\alpha = 30^{\circ}$ |
| 1.5" diam. pile | 1.15 | 1.13 |
| 3.0" diam. pile | 1.30 | 1.27 |

# CHAPTER VI

## CONCLUSIONS

Based on the present experimental investigation on the uplift capacity of vertical and battered piles in sand the following conclusions can be drawn.

1 - The uplift capacity of vertical piles can be calculated by using Meyerhof's theory (15).

2 - Test results indicate that the uplift coefficients of piles in sand decrease slightly with the inclination of the load from $0^{o}$ to $30^{o}$.

3 - The uplift capacity of a single battered pile in sand inclined at an angle $\alpha \leq 30^{o}$ can be computed by using the proposed semi-empirical equation 5.7.

4 - Further research is needed to study the influence of length to depth ratio on the uplift capacity of battered piles and laboratory model test could be extended to cover two-layers sand of different strengths.

## REFERENCES


1 - Awad, A. and Ayoub, A. (1976). "Ultimate uplift capacity of vertical and inclned piles in cohesionless soil", Proc. 5th Budapest Conf. on Soil Mech. and Found. Engr., pp. 221-227.

2 - Begemann, H.K.S.Ph. (1965). "The maximum pulling force on a single tension pile calculated on the basis of results of the adhesion jacket cone", Proc. 6th Int. Conf. on Soil Mech. and Found. Engr., Vol. 2, pp. 229-233.

3 - Bhalla, S.J.S. (1970). "Uplift capacity of inclined piles in sand", M.Engr. Thesis, Nova Scotia Tech. College, Halifax, Nova Scotia, Canada.

4 - Broms, B.B. and Silberman, J.O. (1964). "Skin friction resistance for pile in cohesionless soils", Sols-Soils, No. 10, pp. 33-43.

5 - Caquot, A. and Kerisel, L. (1949). "Traité de Mécanique des sols", Gauthier-Villars, Paris, France.

6 - Caquot, A. and Kerisel, L. (1948). "Table de poussée et butée", Gauthier-Villars, Paris, France.

7 - Coyle, H.M. and Sulaiman, I.H. (1967). "Skin friction for steel piles in sand", Jnl. Soil Mech. and Found. Div., Proc. ASCE, Vol. 93, SM6, pp. 261-278.

8 - Das, B.M. and Seeley, G.R. (1975). "Uplift capacity of buried model piles in sand", Jnl. of the Geotechnical Eng. Div., Proc. ASCE, Vol. 101, No. GT10. pp. 1091-1094.

9 - Downs, D.I. and Chieurzzi, R. (1966). "Transmission tower foundations", Jnl. of the Power Div., Proc. ASCE, Vol. 92, No. P02, pp. 91-111.

10 - Ireland, H.O. (1957). "Pulling tests on piles in sand", Proc. 4th Int. Conf. on Soil Mech. and Found. Engr., London, Vol. 2, pp. 43-46.

11 - Ismael, N.F. and Klym, T.W. (1979). "Uplift and bearing capacity of short piers in sand", Jnl. of the Geotechnical Engr. Div., Proc. ASCE, Vol. 105, No. GT5, pp. 579-593.

12 - Jumikis, A.R. (1962). "Soil Mechanics". D. Van Nostrand Company, Inc.

13 - Kulhawy, F.H. et al. (1979). "Uplift testing of model drilled shafts in sand", Jnl. of the Geotechnical Engr. Div., Proc. ASCE, Vol. 105, No.GT1, pp. 31-47.

14 - McClelland, B. et al. (1969). "Problems in Design and Installation of Offshore Piles", Jnl. of the Soil Mech. and Found. Div., Proc. ASCE, Vol. 95, No. SM6, pp. 1491-1513.

15 - Meyerhof, G.G. (1973). "Uplift Resistance of Inclined Anchors and Piles", Proc. 8th Int. Conf. Soil Mech. and Found. Engr. Moscow, U.S.S.R., Vol. 2, pp. 167-172.

16 - Meyerhof, G.G. and Adams, J.I. (1968). "The Ultimate Uplift Capacity of Foundations", Canadian Geotechnical Jnl., Vol. 5, pp. 225-244.

17 - Muhs, H. (1963). "On the Phenomenon of Progressive Rupture in Connection with the Failure Behaviour of Footings in Sand", Discussion of the Proc. of 6th Conf. on Soil Mech. and Found. Engr., Montréal, Canada, Vol. 3, pp. 419-421.

18 - Nguyen, T.Q. (1984). "Ultimate Bearing Capacity of an Axially Loaded Single Batter Pile in Sand". Ph.D. Thesis in Progress, Concordia University.

19 - Potyondy, J.G. (1961). "Skin Friction Between Soils and Various Construction Materials", Geotechnique, Vol. XI, No. 4, pp. 339-353.

20 - Poulos, H.G. and Davis, E.H. (1980). "Pile Foundation Analysis and Design", New-York, Wiley.

21 - Reese, L.C. and Cox, W.R. (1976). "Pullout Tests of Piles in Sand", 8th Annual Offshore Technology Conf., Houston, Texas, pp. 527-538.

22 - Sowa, V.A. (1970). "Pulling Capacity of Concrete Cast in Situ Bored Piles", Canadian Geotechnical Jnl., Vol. 7, pp. 482-493.

23 - Sulaiman, I.H. and Coyle, H.M. (1976), "Uplift Resistance of Piles in Sand", Jnl. of the Geotechnical Engr. Div., Proc. ASCE, Vol. 102, No. GT5, pp. 559-562.

24 - Terzaghi, K. (1943). "Theoretical Soil Mechanics", New-York, Wiley.

25 - Vesic, A.S. (1970). "Tests on instrumented Piles, Ogeechee River Site", Jnl. of Soil Mech. and Found. Div., Proc. ASCE, Vol. 96, No. SM2, pp. 561-584.

26 - Vesic, A.S. (1967), "A study of bearing capacity of Deep Foundations", Georgia Inst. Tech., Report B-189, Atlanta, Geo.